Ice Flow Line Modeling and Ice Core Data Interpretation: Vostok Station (East Antarctica)

Andrey N. Salamatin*, Elena A. Tsyganova*, Sergey V. Popov**, Vladimir Ya. Lipenkov***

** Kazan State University, Kazan 420008, Russia, Andrey.Salamatin@ksu.ru*
*** Polar Marine Geosurvey Expedition, St. Petersburg 188512, Russia*
****Arctic and Antarctic Research Institute, St. Petersburg 199397, Russia*

Abstract: This work, originally based on a series of the authors' publications [101, 102, 104, 112, 130, 131], considers general questions of ice-sheet flow modeling as related to ice core records interpretation. It reviews the previous results and, using new geographical, geophysical and glaciological data, continues the study aimed at solving the twofold problem of ice core age dating and paleoclimatic reconstructions from the isotopic content measurements in the deep ice cores from Vostok Station located in central East Antarctica, above the vast subglacial lake. The principal idea of the paper is to develop a general approach to past climate investigation by means of an improved thermo-mechanical ice flow line model, involving a wide spectra of supplementary data such as borehole-temperature, radio-echo-sounding reflection layers, and air-bubble measurements.

Key words: ice sheet, ice core records, ice flow line modeling, ice age dating, past climate change

1. Introduction

Numerous evidences confirm a correlation between hydrogen δD (and oxygen $\delta^{18}O$) stable isotope content in solid precipitation and local temperature T_i of atmospheric moisture condensation [11, 12, 18, 27, 50, 133] which, in central Antarctica, is considered to be the cloud temperature at the top of the inversion layer. However, theoretical predictions of the deuterium/inversion temperature transfer function are rather uncertain, and the estimates of its temporal slope C_T generally do not agree with the observed present-day spatial gradients [21, 39, 45, 131]. Obviously, additional independent information on past climate changes is needed to further elaborate and constrain the procedure of processing the unique isotopic signals. This question is closely linked to that of ice core age dating. Actually, simultaneous solution of both problems permits supplementary paleoclimatic analysis of borehole temperature profiles. The non-stationary temperature field in the central part of the Antarctic ice sheet with extremely low accumulation rates remembers [1, 94, 107] recent Milankovich cycles of the past surface temperature variations (geophysical metronome) which, being periodically extended and correlated to the isotopic record, determine [101, 104, 106, 113] the depth-age sequence of the major climatic events (temperature maximums and minimums), i.e. geophysical metronome time scale (GMTS). Furthermore, theoretical investigations and computational experiments show that ice flow line modeling in two-dimensional (2-D) approximation becomes a useful tool for ice age predictions in central parts of an ice sheet if the model parameters are constrained by *a priori* chronological information [74, 75, 137]. From this point of view, GMTS can be considered [3, 34, 35, 112] as an important and statistically significant set of the so-called orbitally tuned age markers (control points). Another independent source of age markers may be provided for future studies by the local insolation proxy properties of atmospheric air trapped in ice [6, 90]. Once the ice age-depth relationship is introduced, fitting the 2-D thermo-mechanical simulations to the borehole temperature measurements reliably constrains the transformation of the ice core isotope time series into the history of ice-sheet surface temperature (T_s) variations [101, 104, 113, 130].

However, the above general strategy of paleoreconstructions is not complete. The borehole thermometry does not directly constrain the inversion (condensation) temperature T_i which determines the water-vapor equilibrium pressure in clouds conventionally correlated [97] in the central Antarctica to solid (snow) precipitation. Hence, past temporal variations of the ice accumulation rate b, the principal climatic input of the ice-sheet dynamics, remain highly uncertain. The use only of a local set of the ice age-depth correlation points for tuning a multi-parameter ice-flow line model does not account for geographic peculiarities of environmental conditions and does not permit simulation of a realistic spatial flow pattern. This is especially important when, as in the case of the Vostok ice core, the drilling site is not a dome summit, but is located relatively far from the ice divide above the vast subglacial lake [46]. The situation can be substantially improved if the ice core data on geometrical properties of air inclusions are involved in the paleoclimatic studies. Based on a self-similarity of dry firn structures at pore closure [30], a new constraint on the past accumulation rates was proposed in [55] and has been later discussed in [124]. The original conclusion is that the total bubble number density is

inversely proportional to the mean ice-grain volume at the close-off and, thus, due to normal grain growth in snow and firn, must be related to the local climatic conditions (b and T_s) of ice formation. Recent studies [103, 105] of the snow/firn densification process result [56] in developing an explicit semi-empirical equation which links relative past accumulation rates along the flow line to the bubble number measurements and the ice-sheet surface temperatures. Furthermore, extensive radio-echo sounding (RES) observations were carried out from the ice-sheet surface by the Polar Marine Geosurvey Expedition (PMGE) in the vicinities of Vostok Subglacial Lake (VSL) in 2004-2006. In particular, the bedrock relief and distinct isochronous (reflection) layers with the ice age up to ~220 kyr were detected in RES profiling over the 106-km traverse along the ice flow line upstream of Vostok Station. The described complex of experimental and theoretical works for the first time has provided various paleoclimatic, glaciological, and geophysical data from Vostok area to attempt a joint self-consistent analysis based on the ice flow line modeling and aimed at simultaneous solving the twofold problem of ice-core age dating and paleoclimatic reconstructions from ice-core isotopic records.

Aside from ice-sheet dynamics and formation of paleoclimatic signals, the study of heat transfer along ice flow lines starting from Ridge B and passing across the lake and Vostok Station is of primary importance for our understanding the gas (air) and water exchange between the ice cover and the subglacial water basin, as well as for investigation of biological processes and possible origins of microbial life in the lake (e.g. [77, 117]). Non-stationary temperature fields determine the ice accretion and melting rates at the ice - water interface [76, 77, 109, 125, 130] and, as a consequence, lake salinity and the rates of air accumulation in the lake in the forms of dissolved air and air hydrates [54, 68]. Temperature conditions along ice particle trajectories in the glacier directly control the air hydrate crystal growth [108, 132] and the state of micro-organisms transported through the glacier from its surface towards the lake.

With this in mind, we, first, review and compare after [131] different approaches to paleoclimatic interpretation of ice core isotopic records, borehole temperature profiles and discuss existing uncertainties in ice age datings of different origins at Vostok. Then, in a continuation of [100, 130], an improved sophisticated ice flow line thermo-mechanical model is elaborated for simulating the ice sheet dynamics and temperature field along the Vostok flow line with account of the ice deformation within the bedrock - subglacial lake transition zone and the ice accretion at the glacier bottom over the lake. Recent RES observations, updated geographic, geophysical and glaciological data are summarized. Supplementary information about past accumulation rates deduced from the bubble density measurements [56] is also described. Finally, the general strategy and results of the newly performed computational experiments are discussed to present the re-examined glaciological time scale for the Vostok ice core and resultant paleoclimatic reconstructions.

2. Paleoclimate in the Antarctic ice memory. Previous studies

2.1 Isotope content of ice

Although we conventionally refer to the correlation between stable isotopes in solid precipitation in central Antarctica and local inversion (condensation) temperature T_i, it should be noted that the isotopic content of deep ice cores can differ from that of the fresh snow due to the surface snow metamorphism and mass exchange with the atmospheric moisture. The sublimation and recrystallization effects in snow and firn (e.g. [28, 49, 115]) are primarily controlled by the near-surface glacier temperature T_s which, in central Antarctica, is significantly lower than T_i due to the developed inversion strength. As a result, the stable isotope content in ice cores corresponds to a certain apparent temperature, which, in general, may not coincide with any of the instrumentally measured values. Nevertheless, it is still assumed that the temperature fluctuations themselves deduced from the isotopic content variations do not differ much from those of the effective temperature of the atmospheric moisture condensation. The detailed analysis of the present-day isotope-temperature correlations based on meteorological observations, measurements in pits, and borehole thermometry for the recent 50 years [21, 23, 24, 59] confirms this conclusion. Importance of the deuterium excess $d_{ex} = \delta D - 8\delta^{18}O$, as a derived paleosignal, and its relation to thermodynamic conditions of moisture formation in the evaporation zone, e.g., source temperature T_w, have been demonstrated in [38, 42, 43, 79]. A complete set of the ice core isotopic data from the deep borehole at Vostok Station to a depth of 3310 m and its detailed analysis are presented in [135]. Fig. 1 depicts results of these measurements together with the parabolic mean-square spline approximation of the ice isotope content fluctuations versus depth. Substantially more detailed experimental studies on the Vostok ice core deuterium content to 3350 m were performed and summarized earlier in [78].

The advantage to employ simultaneously both isotopic signals, δD and d_{ex}, in paleoclimatic reconstructions and the necessity to deduce past temperature variations at a site of solid (snow) precipitation together with those in the moisture-evaporation zone was shown in [14, 134]. Linear relationships were proposed to determine the relatively small temperature perturbations:

$$\Delta\delta D = \gamma_i \Delta T_i - \gamma_w \Delta T_w + \gamma_m \Delta\delta^{18}O_m ,$$
$$\Delta d_{ex} = -\beta_i \Delta T_i + \beta_w \Delta T_w - \beta_m \Delta\delta^{18}O_m . \quad (1)$$

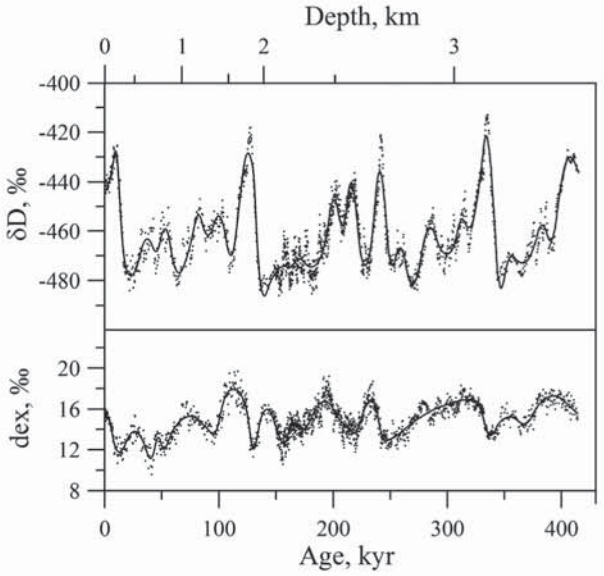

Figure 1: Deuterium content and deuterium excess measurements in Vostok ice core vs. depth [135] (dots) and their spline approximations (solid lines).

Here $\delta^{18}O_m$ is the ocean water oxygen isotope content, Δ means the deviation of the characteristics from their contemporary values; γ_i, γ_w, γ_m, β_i, β_w, β_m are the regression coefficients, which are introduced as positive values and describe the climatic links of the site under consideration with the processes of atmospheric circulation.

At a given correction for the isotopic content of sea water $\Delta\delta^{18}O_m$ [4, 36, 78, 123], the system of the algebraic equations (1) allows to calculate variations of the climatic parameters ΔT_i and ΔT_w from the isotope content of ice $\Delta\delta D$ and Δd_{ex}. If, as a first approximation, a proportionality of the temperature fluctuations is assumed [48], i.e. $\Delta T_w \approx r_{wi}\Delta T_i$, then the first of equations (1) reduces to the relationship [41] traditionally used in paleoreconstructions for estimation of the inversion temperature variations

$$\Delta T_i = (\Delta\delta D - \gamma_m \Delta\delta^{18}O_m)/C_T\,, \quad C_T = \gamma_i - \gamma_w r_{wi}\,. \qquad (2)$$

At the same time, in accordance with [97], the amount of precipitation (ice accumulation rate b) in Antarctica is correlated with the water vapor saturation pressure in clouds and can be calculated after [94, 95] as

$$b = b_0 \bar{b}(s) \exp(\eta_b \Delta T_i), \qquad (3)$$

where b_0 is the present-day value of the accumulation rate at the site under consideration ($s = s_0$), $\bar{b}(s)$ is the normalized spatial distribution of the accumulation rate along a reference ice flow line with the distance s counted from the ice divide.

The coefficient η_b in Eq. (3) can be expressed [95] via the present-day condensation temperature (the cloud temperature T_{i0} at the top of the inversion layer) $\eta_b = 6148.3/(273.15 + T_{i0})^2$, and at $T_{i0} = -38.0 \pm 0.6$°C [21] $\eta_b \approx 0.112$°C^{-1}. Close estimates of $\eta_b \sim 0.10$-0.14°C^{-1} follow from the geographical dependence of the accumulation rates on the isotope content of the surface snow layer in East Antarctica along the traverses "Mirny Observatory - Vostok Station" [21, 22, 53] and "Syowa Station - Dome Fuji" [114].

The large inversion strength, $T_s - T_i$, over the Antarctic Plateau generally implies the necessity to develop special approaches for reconstruction of the surface temperature variations ΔT_s in the past. Based on the present-day spatial distributions of the surface and inversion temperatures, Jouzel and Merlivat [42] proposed a linear proportionality between ΔT_s and ΔT_i:

$$\Delta T_s = \Delta T_i / C_i\,. \qquad (4)$$

Eqs. (1)-(4) form a theoretical basis for paleoreconstructions from the ice core isotopic data stored in the Antarctic ice sheet memory. The principal problem of their practical employment is in reliable constraining of the coefficients in this paleoclimatic model. In particular, the reviews [14, 48, 102, 134, 135] are devoted to the validation of Eqs. (1). A summary of results obtained in these publications is presented in Table 1. The simplified Rayleigh-type model for the atmospheric moisture condensation and isotopic fractionation in air masses moving along a single trajectory [10, 18, 26, 38, 42, 69] was used in [14, 134] to calculate the isotopic composition of precipitation in Central Antarctica. Although this model omits the evaporative recharge of the air mass by moisture from the ocean, the derived values of the γ and β coefficients (variant V-1) were, partly, confirmed by simulations on the basis of global atmospheric circulation models (GCM) and were compared with the direct geographical observations. In [102], the Rayleigh scheme of the isotopic fractionation was re-examined to take additionally into account the feedback between the isotope content of the moisture in the air leaving the low-altitude evaporation zone and the influx of the less moist and isotopically depleted air coming to the source area. It is important that the computations (variant V-2) revealed a substantially higher sensitivity (coefficient β_i) of the deuterium excess d_{ex} to the condensation temperature T_i at a precipitation site. A new "intermediate" model for the formation of the isotopic composition in precipitation in Antarctica was proposed by Kavanaugh and Cuffey [48] as a generalization of [25, 32, 47]. This model includes the turbulent convective mixing in the longitudinal direction and the evaporation (recharging) from the ocean. However, the vertically integrated uniform profiles of all important characteristics (temperature, humidity, isotopic ratios etc) were assumed, implying infinitely fast altitudinal air and moisture mixing. Thus, the two simplified approaches [48] and [102] to the description of the isotopic fractionation in the global hydrological cycle can be considered as limiting scenarios with respect to the vertical water-vapor transfer effects. Computational experiments performed by Kavanaugh and Cuffey [48]

Table 1. Coefficients of the isotope-paleoclimate models (1)-(4) and (6) *

Parameter	Isotope fractionation models			Meteorol. data [21]	Geographic data	Ice flow models	Thermo-mechanical models
	V-1 [14]	V-2 [102]	V-3 [48]				
γ_i, ‰°C^{-1}	10.6	10.3	7.5-9.5		9-13		
γ_w, ‰°C^{-1}	3.7	2.8-3.6	2.5-2.8				
γ_m	4.8	4.5-4.7	4.5-4.6				
β_i, ‰°C^{-1}	0.75	1.72-1.38	0.79-1.1				
β_w, ‰°C^{-1}	1.3	1.66-1.76	1.3-1.6				
β_m	2.8	3.0-2.9	3.0				
C_T, ‰°C^{-1}			5.0-7.5	6.2±1.1	13±1[21] 9 [41,78]	7.7±1.1 [3] 6.7 [34] 6.0-6.3 [112]	3.6-7.3 [101,104,113] 6.1-6.5 [130,131] **6.1**
C_i				**0.7-0.8**	0.45-0.52 [21] 0.67 [42]		0.7-0.79 [130,131] **0.79**
C_iC_T, ‰°C^{-1}					6.4±0.2 [15,22] ~6 [62]		2.9-5.1 [3,101,104,113] 3.6±1.0 [59] 4.2-4.8 [130,131] **4.8**
α_p							0.14-0.31 [3,101,104,113] 0.11-0.12 [130,131] **0.06-0.12**

* The most reliable recommended estimates are given in bold

to study the general sensitivity of the isotope content of ice deposits in the Vostok Station area to the global temperature changes did not result in unique estimates for the coefficients γ_i, γ_w, and C_T in Eqs. (1) and (2) (variant V-3, Table 1) and demonstrated a strong dependence on possible moisture exchange regimes. Systematically lower estimates of γ_i and γ_w at intermediate values of β_i were obtained in this case in comparison with the variants V-1 and V-2, while, as emphasized in [14, 48], the coefficients γ_m and β_m were reliably determined. It should be noted after [45] that, in accordance with this work, γ_m in Eqs. (1) and (2) is equal to 4.6 instead of 8 traditionally assumed earlier.

The difference in the estimates of the principal coefficients γ_i, γ_w and β_i, β_w is rather significant and, as shown in [102], can lead to the substantial uncertainty in paleoreconstructions. Fig. 2a evidently illustrates this conclusion and demonstrates how different the deduced fluctuations of ΔT_i and ΔT_w can be, depending on a chosen combination of the coefficients in Eqs. (1).

Unfortunately, numerous attempts to use GCMs were focused [21, 45] mainly on Eq. (2) describing temporal variations of the condensation temperature in order to investigate the difference of the combined coefficient C_T from the corresponding spatial (geographic) isotope/inversion temperature slope. In particular, for the Vostok area conditions, a 30% reduction of C_T in comparison with its geographic analogues can not be excluded [39, 45]. Such deviations are also in agreement with the general relations (1). For example, if the contemporary latitudinal distributions of isotopes are formed by air masses coming from one source, at $\Delta T_w = 0$, the spatial C_T slope in Eq. (2) should be identified with γ_i. On the other hand, in accordance with the predictions of isotopic fractionation models (see variants V-1, 2, 3, Table 1), the ratio C_T between the temporal variations of $\Delta\delta D - \gamma_m \Delta\delta^{18}O_m$ and ΔT_i for $r_{iw} \sim 0.5$-1 in Eqs. (2) will be 15-35% lower.

Available meteorological observations and special measurements in pits in vicinities of Vostok Station were analyzed and summarized in [21]. The deduced statistically valid regression coefficients of the correlation between the seasonal condensation temperature oscillations and the isotopic composition of precipitation (C_T) during the year 2000, as well as between long-term (over 50 years) annual inversion temperature variations and the air temperature near the ice sheet surface (C_i) are presented in Table 1. Let us note that seasonal changes in the inversion temperature and the surface air temperature give almost a two times lower value of C_i which agrees with the earlier estimate [80]. This difference is explained by the seasonal character of the inversion strength [21].

Geographic data on the present-day distribution of the isotopic content in surface snow over Antarctica and the correlation between the isotopes and the surface temperature, including measurements [15, 62], were analyzed in [21, 22]. For East Antarctica, the ratio between the deuterium content variations and the near-surface air temperature was determined to be $C_iC_T \approx 6.4\pm0.2$‰°C^{-1} and is in close agreement with the value of 6.04‰°C^{-1} from [62] and with the estimate [114] obtained for the oxygen isotopes corresponding to $C_iC_T \approx 6.8$ ‰°C^{-1} for deuterium. According to [42], the spatial relationship (4) between the inversion and surface temperatures in Antarctica is characterized by the coefficient $C_i = 0.67$. Consequently, the traditionally used estimate of $C_T \approx 9$‰°C^{-1} [78] directly follows [41] from [62]. However, as shown in [21], the inversion temperature is close to that of the atmospheric moisture condensation in clouds only in the central regions, and spatial variations of the condensation temperature are described by noticeably lower values of $C_i \approx 0.45$-0.52,

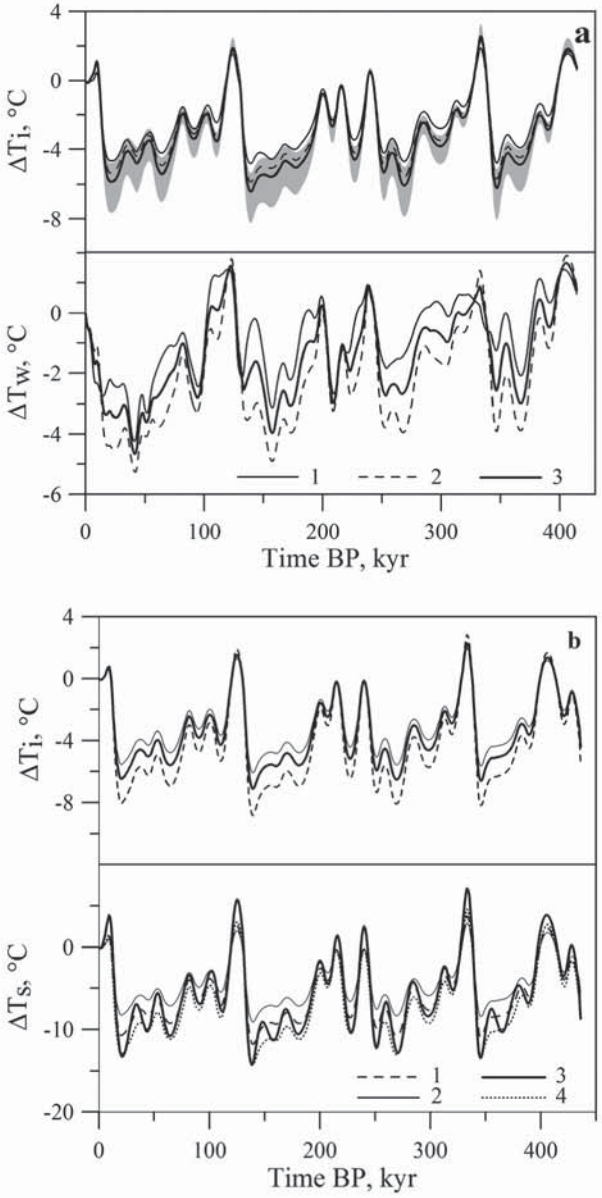

*Figure 2: Uncertainty of paleotemperature reconstructions. (**a**) Variations of the inversion temperature ΔT_i and moisture-source temperature ΔT_w deduced from Eqs (1) at the mean values of the coefficients for variants V-1 – V-3 in Table 1 (cures 1-3, respectively), the shaded area is the uncertainty of the inversion temperature reconstructions in V-3 [48]. (**b**) Variations of the inversion and surface temperatures ΔT_i and ΔT_s from Eqs (2) and (4) at the mean values $C_T = 6.2$ ‰°C^{-1}, $C_i = 0.75$ for meteorological observations [21] and ice flow modeling [112] (curves 1), for geographic estimates $C_T = 9$ ‰°C^{-1}, $C_i = 0.67$ [41,42] (curves 2) and from Eqs (2) and (6) after [3] at $C_T = 7.7$ ‰°C^{-1}, $C_iC_T = 3.8$ ‰°C^{-1} with $\alpha_p = 0.18$ (curves 3) and $\alpha_p = 0$ (curve 4).*

resulting in substantially higher estimates of $C_T \approx 13\pm1$‰°C^{-1} for the condensation temperature.

Thus, the correlations between contemporary spatial distributions of the isotope composition of surface snow and temperature in Antarctica can not be directly used in paleoreconstructions of climatic time series even in the simplified procedure (2)-(4). Totally, the geographic estimates of the slope $C_T \approx 9$-13‰°C^{-1} are not in contradiction with the theoretical predictions of the coefficient $\gamma_i \approx 7$-11‰°C^{-1} in Table 1. However the observational data do not specify the calculated values. At the same time, as can be seen from Table 1, the meteorological observations of the short-term changes in the inversion temperature and the isotopic composition in precipitation at Vostok Station [21], in spite of their high uncertainty, give the estimates of the temporal slope in Eq. (2) close to the model results $C_T \approx 5$-7.5‰°C^{-1} [48]. Furthermore, it follows from [21] that the difference between the temporal variations of the inversion temperature (apparent condensation temperature) and the surface temperature at Vostok Station (see Table 1) is substantially less ($C_i \approx 0.7$-0.8) in comparison with their spatial distributions ($C_i \approx 0.67$ or even 0.45-0.52).

2.2 Ice sheet temperature field

The reviewed studies support very high informativeness of the ice core isotopic records form deep boreholes drilled in central parts of Antarctic ice sheet. However, it becomes clear that additional independent data on the past climate changes should be involved in the interpretation of these unique paleoclimatic signals to further validate and calibrate the transfer functions (1)-(4). This task does not exhaust the whole problem of paleoreconstructions as a procedure of deriving the past temperatures and precipitation. Another closely related question is the ice core age dating. A simultaneous solution of these two problems permits supplementary paleoclimatic analysis of borehole temperature measurements [104, 106].

Let us discuss this point in more details. The first computational experiments [1, 16, 94] showed that borehole temperature profiles in the large ice sheets on our planet contain the information about past temperature fluctuations at the glacier surface. Further studies [13, 17, 37] of the heat transfer processes in the central regions of Greenland ice sheet with relatively high accumulation rates and moderate ice thickness allowed directly to infer the detailed surface temperature variations over the recent 25-30 kyr from the temperature surveys in deep boreholes and made it possible to analyze the relationship between the temperature and the isotope content of ice. The far past history was "forgotten".

As shown in [101, 104, 106, 107], in contrast to Greenland, the non-stationary temperature field in the centre of Antarctic ice sheet with extremely low accumulation rates and maximum ice thickness remembers distinguishable local temperature perturbations, induced by the recent astronomic Milankovich cycles with the eccentricity, obliquity, and precession periods of $t_1 = 100$, $t_2 = 41$, and $t_3 = 23$, $t_4 = 19$ kyr dominating in the Pleistocene climate in central Antarctica [4, 36, 141]. However, more or less

reliable information about the details of short-term temperature fluctuations in the past on time scales of 3-5 kyr is lost. This restricts substantially the applicability of direct inverse methods for paleoclimatic reconstructions on the basis of borehole temperature measurements alone [72, 101]. Yet, representing, in accordance with the Milankovich climate theory, the surface temperature fluctuations as a superposition of harmonic oscillations of the fixed frequencies $\omega_j = 2\pi/t_j$ ($j = 1,\ldots, 4$),

$$T_s(t) = T_{s0} + \sum_{j=1}^{4}\left[A_j\left(\cos(\omega_j t) - 1\right) - B_j \sin(\omega_j t)\right], \quad (5)$$

it becomes possible to find [3, 101, 104, 106, 107, 113] the contemporary ice sheet surface temperature T_{s0} and the cosine and sine amplitudes A_j and B_j of the four Milankovich cycles by minimizing the standard deviation (SD) between simulated and measured temperature profiles. Here t is the time counted from the far past ($t < 0$, and $t = 0$ is the present moment).

Various borehole thermometry data of different quality and observational depths were used in the above cited papers. Despite noticeable deviations of inferred amplitudes, the geophysical metronome (5) reliably reproduced (with accuracy of ~1-2 kyr) the ages of the major climatic events (temperature maximums and minimums) at the glacier surface. From this point of view, it is of principal importance that the same paleoclimatic extrema are clearly distinguished in the smoothed variations of the deuterium content in ice cores versus depth (Fig. 1). Consequently, although the absolute temperature transitions between different climatic stages are not precisely determined, the ice age dating seems to be rather reliable. The resulting sequence of the depth-age correlation points was called [104] the geophysical metronome time scale (GMTS). The age markers uniformly distributed versus depth can be used to deduce an estimate for the coefficient C_T in Eq. (3) which determines the accumulation rate, the principal climatic input of ice sheet flow models. The value of C_T must be in agreement with GMTS on average, resulting in the minimum standard deviation of the simulated (so-called glaciological) ice core time scale from the given set of control points. Preliminary fitting was performed on the basis of a simplified ice flow model [3, 34]. The obtained respective values of $C_T \approx 7.7\pm1.1$ and $6.7‰°C^{-1}$ do not contradict with the other estimates [21, 48] in Table 1. However, the coefficient η_b in Eq. (3) was determined [95] only approximately, and its error is automatically included into the deduced value of the C_T parameter.

Once the ice core time scale is introduced, the borehole temperature measurements can be employed [94] for calibration of Eqs. (1), (2) and (4) which transform the isotopic time series into temporal variations of the ice sheet surface temperature T_s as the principal climatic factor of the model input. For the simplified relations (2) and (4), only T_{s0} and the product C_iC_T (or C_i) must be tuned. However, the analysis of the high-precision temperature profile measured by Yu. Rydvan [106] at Vostok Station in 1988 to a depth of 1900 m showed [104] that, at least, the recent climatic fluctuations ΔT_s contained a selectively amplified (supplementary) precession signal δ_p which could not be reproduced simply by scaling of the inversion temperature variations ΔT_i in Eq. (4). To account for this, although small, correction, a generalized form of Eq. (4) was proposed

$$T_s = T_{s0} + \Delta T_i/C_i + \delta_p(t), \qquad \delta_p(t) = \alpha_p \sum_{j=3}^{4}\left[A_j\left(\cos(\omega_j t) - 1\right) - B_j \sin(\omega_j t)\right], \quad (6)$$

where α_p is the scaling factor of the precession components of the local geophysical metronome (5) [3, 101, 104, 113].

The best-fit values of the product C_iC_T and the α_p coefficient were first inferred [104] from Rydvan's temperature profile [106] and in two limiting cases were found to be $C_iC_T \approx 4.8\pm0.3$ and $4.2\pm0.3‰°C^{-1}$, $\alpha_p \approx 0.29$ and 0.14, respectively. Less accurate stacked temperature profile down to a depth of 3590 m was used in [101, 113] and lead to lower estimates of $C_iC_T \approx 3.3$ and $2.9‰°C^{-1}$ at $\alpha_p \approx 0.24$ and 0.31. Preliminary results of the new continuous temperature survey performed by R. Vostretsov at the end of 1999 to a depth of 3620 m in the record borehole at Vostok Station (almost two years after the drilling operations had been stopped) were analyzed in [3]. They gave intermediate values of $C_iC_T \approx 3.8\pm0.1‰°C^{-1}$ and $\alpha_p \approx 0.18$. In all the above cited papers, an approximate quasi-one-dimensional heat transfer model [101, 106, 107] was used for simulating the ice-sheet temperature field in central Antarctica. In addition, it becomes clear that the inferred values of the tuning coefficients are substantially influenced by accuracy of temperature measurements. The bounds of the deduced parameters in Eqs. (6) are presented in Table 1. They are in agreement with the estimate of $C_iC_T \approx 3.6\pm1.0‰°C^{-1}$ inferred in [59] from borehole temperature observations in a 100-meter surface layer at Vostok Station over the last 50-year period. It can easily be seen that in all these cases the use of the direct measurements [21] of the C_i coefficient or its geographic analogue [42] leads to the calculated values of C_T comparable to other independent estimates of this parameter in Table 1 except for the much higher geographic slopes. It should be mentioned that these estimates of C_T do not take into account the supplementary precession signal δ_p in the relationship (6) which slightly increases the amplitude of temperature oscillations at the ice sheet surface in comparison with the simplified equation (4).

Various limiting cases of the inversion and surface temperature fluctuations ΔT_i and ΔT_s reconstructed from the ice core deuterium record (see Fig. 1) on the basis of Eqs. (2), (4) and (6) calibrated by the temperature measurements at Vostok Station are shown in Fig. 2b.

These results agree with the calculations of ΔT_i from Eqs. (1) in Fig. 2a, although they also demonstrate a significant diversity. In particular, the decrease in the inversion temperature (effective condensation temperature) determined by meteorological observations and the change in the ice sheet surface temperature inferred from the borehole temperature profile for the LGM at Vostok Station are 30-50% larger than the corresponding estimates based on the geographic data. The impact of the precession signal δ_p in Eqs. (6) is revealed (see doted curve in Fig. 2b) in more pronounced (by 2-2.5°C) climatic maximums in the surface temperature.

3. Age of the Vostok ice core. Uncertainties and problems

3.1 Ice age datings of different origins

There is no universal and/or standard procedure to determine depth-age relationships in polar ice sheets at sites of deep drilling. The latter question is of primary importance for the deep ice core retrieved from the Antarctic ice sheet at Vostok Station [78]. Possible applicability of sophisticated 2-D and 3-D thermomechanical ice flow models [95, 96] for solving this problem significantly suffers from inevitable uncertainties in initial and input data, mainly in glacier bottom conditions and past accumulation rates. This was the principal obstacle limiting the accuracy of earlier simulations and ice age predictions by ~15-20 kyr. Nevertheless, theoretical studies and computational experiments [74, 75, 137] show that the modeling of ice sheet dynamics becomes a useful tool for the ice age prediction in central areas of large ice sheets if *a priori* chronological information is used to tune the model parameters. Not being free from their own specific errors, different sources of age markers and dated time series can, yet, be considered as reliable constraints if all together they deliver statistically valid and independent estimates of ice age at various depth levels. The inverse Monte Carlo sampling method (e.g. [70, 71, 128]) is especially helpful in this case [74] to fit the ice-sheet model on average, uniformly versus depth, although without putting much weight on local (high-frequency) fluctuations of the simulated depth-age curve caused by uncertainties in environmental conditions, reconstructed ice accumulation and other paleoclimatic characteristics. From this point of view, as a first approximation, even simplified ice flow models (e.g. [3, 34, 35, 110, 112]) may be quite appropriate to incorporate the principal laws of ice-sheet dynamics into the ice core dating procedure.

Among different depth-age relationships developed for Vostok, the geophysical metronome time scale (GMTS) [104, 106] extended in [3, 101, 113] to the maximum depth 3350 m of the Vostok ice core isotope record covering four interglaciations represents the so-called orbitally tuned chronologies. As explained in section 2, it is based on the correlation of the isotopic temperature signal with the geophysical metronome, i.e. Milankovich components of the local surface temperature variations in the past inferred from the borehole temperature profile. Possible errors and uncertainties of GMTS were discussed in [101, 104], and its overall average accuracy was estimated as ±3.5-4.5 kyr. Orbital ice age control points used in [74,75] as model constraints coincide (to within ±2 kyr) with the corresponding GMTS ages.

Another paleotemperature-proxy signal spanning over more than 500,000 years is available from the calcite core in Devils Hole (DH), Nevada [139, 140]. The principal advantage of this $\delta^{18}O$ record is that the dense vein calcite provides a material for direct uranium-series dating [63] with the relative standard errors of about 1.5-2%. In addition, the signal may be influenced by different hydrological factors. In particular, a systematic underestimation of the determined ages on the order of several (two) thousands of years may take place due to the ground-water travel time through the aquifer [51, 139]. Nevertheless, the correlation of the Vostok ice core deuterium-depth signal with the Devils-Hole record (see U.S. Geological Survey Open-File Report 97-792 at http://pubs.water.usgs.gov/ofr97-792) can also be considered as an independent approach to dating long paleoclimate archives from central Antarctica [51].

Note, that we do not discuss here a possibility (e.g. [7, 123]) to employ various gas studies of Vostok ice cores for relative dating (correlation) with other Antarctic, Greenland or deep-sea core climatic records, because of inevitable additional errors which arise in this case from the uncertainty in the gas-ice age difference preventing better constraints on the ice age.

3.2 Glaciological and average time scales

The best-guess glaciological time scale simulated in [75] was mainly based on the RES data by Siegert and Kwok [118] and is designated as GTS-I after [131].

The principal goal of [112] was (1) to combine the GMTS and DH sources of chronological information (70 age markers of climatic events totally) in order to constrain ice flow model parameters, reducing to minimum systematic errors in the glaciological time scale based on simulations of ice sheet dynamics in the vicinities of Vostok Station and (2) to deduce an average age-depth relationship consistent with different approaches to ice core dating within the upper 3350 meters. For the grounded part of the ice sheet, the reference flow line passing through Vostok Station was drawn perpendicular to the surface elevation contours [119], and the ice flow tube configuration was approximately determined after [117, 118, 127]. Over the lake, the flow line was continued in accordance with the observations [5, 125]. A monotonically increasing spatial distribution of the normalized mass balance $\bar{b}(s)$ in Eq. (3) was schematically taken as similar to the smoothed accumulation rate profile along the traverse to Vostok [53] with account of the mass-balance enhancement factor 1.65 estimated [40] for Ridge B at the location of the Dome B ice core. The present-day ice-sheet thickness at Vostok was assumed

to be 3755 m after [64]. The bounds for the mean recent accumulation rate at Vostok were determined on the basis of [2, 22, 24].

Tarantola's theory [128] and the Monte Carlo (random walk) sampling procedure [70, 71] were employed in [112] to solve the inverse problem and to find the optimal model parameters among which the principal ones were the present-day accumulation rate b_0 and the deuterium/inversion temperature slope C_T in Eqs. (2) and (3). The modelled best-guess ice age-depth distribution is called GTS-II. Its standard deviations from GMTS and DH age markers were estimated as ~4.5 and 7 kyr, respectively. In general, GTS-II can be considered as another source of ice age estimates with minimum systematic error, though containing its own independent short-term distortions which are the attributes of the model imperfectness and uncertainties of the geographic input. This finally suggested construction of an average time scale for the Vostok ice core down to a depth of 3350 m based on GTS-II and linear interpolations of GMTS and DH age-depth correlation points. The averaging procedure was performed iteratively with the weights taken inversely proportional to standard deviations of the basic chronologies from the resulting smoothed average curve. The highest weighting coefficient (accuracy) of 44% was determined for the best-fit glaciological time scale GTS-II; the weights of 38 and 18% were found for GMTS and DH age markers, respectively, in accordance with their statistical validity. The average time scale is consistent with all three basic age-depth relationships within the standard deviation bounds of ±3.6 kyr which correspond to the upper estimate of the age uncertainty. Actually, the weighted mean standard deviation of the averaged chronologies (i.e., ±2.2 kyr) is thought to be a more reliable measure of the accuracy of the resulting mean ages. Although one may argue that the simplified ice flow model, high uncertainties in the environmental conditions and the use of DH isotope time series do not give any advantage to the average time scale, the latter age-depth relationship, still, can be regarded as a common reference basis for intercomparison of different datings for the Vostok ice core.

The tuning of the ice sheet flow model was performed in [112] for the climatic input described by Eqs. (2) and (3), and, at the correction factor of $\gamma_m = 8$ for the sea-water isotopic composition, the best-fit values of the temporal isotope/inversion temperature slope were inferred as $C_T \approx 6.0\text{-}6.3$‰°C^{-1} with the standard deviation of about 0.6‰°C^{-1}. The use of the re-examined value of $\gamma_m \approx 4.6$ in Eq. (2) instead of 8 reduces the estimate of C_T by ~0.4‰°C^{-1} without any influence on the ice dating. The obtained result agrees with the other data presented in Table 1. The best-fit present-day accumulation rate was found at its lower bound 2.15 cm yr^{-1} and matches with the mean value 2.23 ± 0.03 cm yr^{-1} calculated for the recent 190 years from the depths of the Tambora eruption layer measured at Vostok in 9 shallow boreholes and deep pits [24].

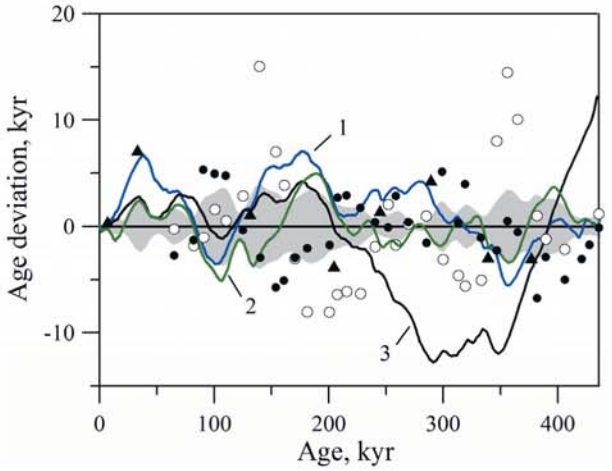

Figure 3: Comparison of the average time scale for Vostok ice core [112] (zero line) with the best-guess glaciological time scales GTS-I [75], GTS-II [112] and GT-4 [78] (curves 1-3, respectively). The shaded area is the confidence interval of the running averaged ages. Filled and open circles are the GMTS and DH age markers, triangles are the control points used in [75].

The average time scale (zero reference line) is compared in Fig. 3 with the previously used glaciological time scale GT-4 [78] and the best-guess age-depth relationships GTS-I and II developed through the ice sheet model constraining in [75] and [112]. The GMTS and DH control points are shown by empty and solid circles, respectively. The shadowed area in the figure represents the confidential interval for the average time scale with the boundaries determined as the standard deviations of the three basic chronologies from the mean ages. As can be seen, an obvious progress has recently been achieved in ice core age dating at Vostok. It is also important that the above cited papers [75, 112] used similar modeling approaches and inverse methods. The standard deviation between GTS-I and II is about 3.3 kyr on average and is comparable with the estimated errors of the average time scale. However, local discrepancies between GTS-I and GTS-II ages still reach 7-8 kyr and are mainly caused by differences in the initial geographic and paleoclimatic data. New studies and special sensitivity tests [130, 131] additionally confirm that the reliability of ice core age dating and paleoreconstructions depend substantially on accuracy of thermo-mechanical modeling and quality of input (environmental) information.

4. Vostok flow line modeling

4.1 Ice flow tube geography and RES data

As mentioned above, environmental ice sheet flow conditions previously used in [75, 112, 130, 131] were rather uncertain and in some cases even schematic.

In this study, the Antarctic ice sheet surface elevation map of the Lake Vostok vicinities (Fig. 4) is based on the ERS-1 satellite altimetric data [60, 92] adapted after

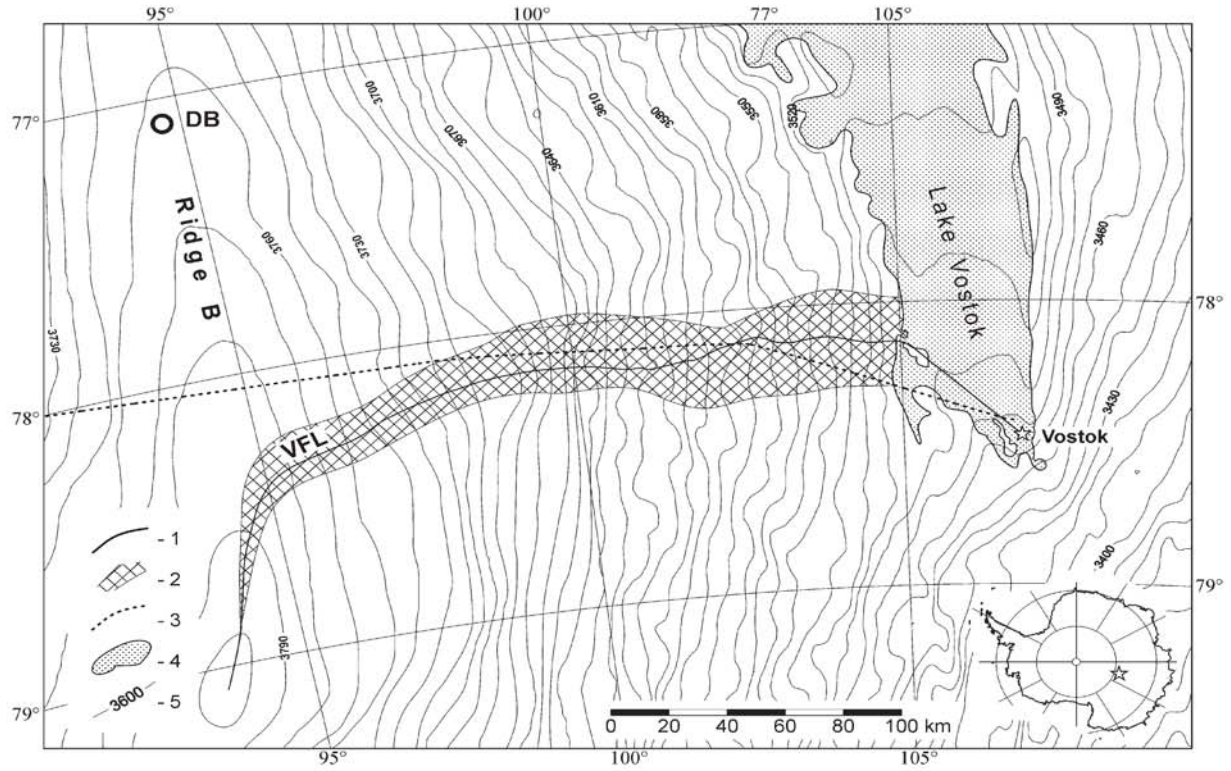

Figure 4: Surface elevation map of Lake Vostok vicinities [60, 92] adapted after [129]. 1- Vostok ice flow line (VFL); 2- ice flow tube; 3- SPRI/NSF RES route [19, 98]; 4- Lake Vostok water table [83]; 5- elevation contours with 10-m spacing.

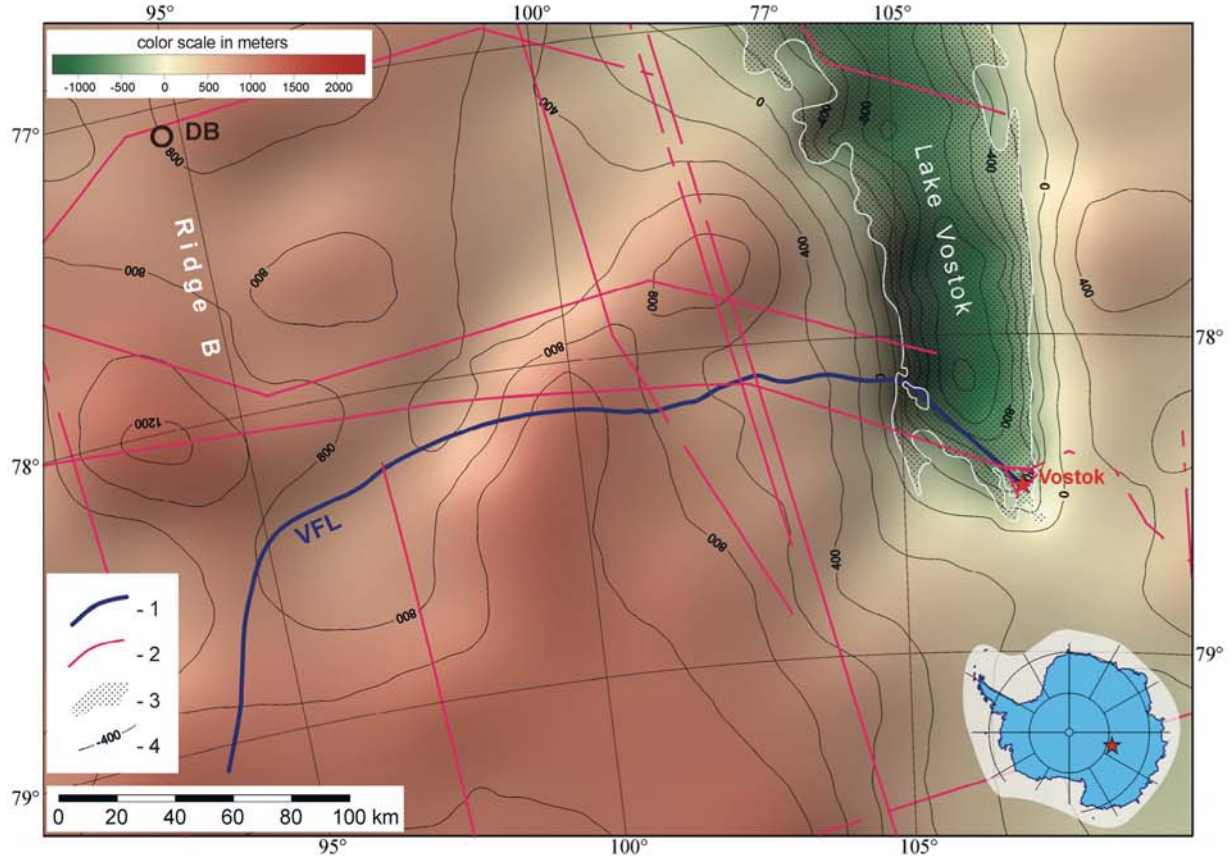

Figure 5: Bedrock topography map of Lake Vostok vicinities after ABRIS project [82]. 1- Vostok ice flow line (VFL); 2- SPRI/NSF RES routes [20, 98]; 3- Lake Vostok water table [83]; 4- elevation contours with 200-m spacing.

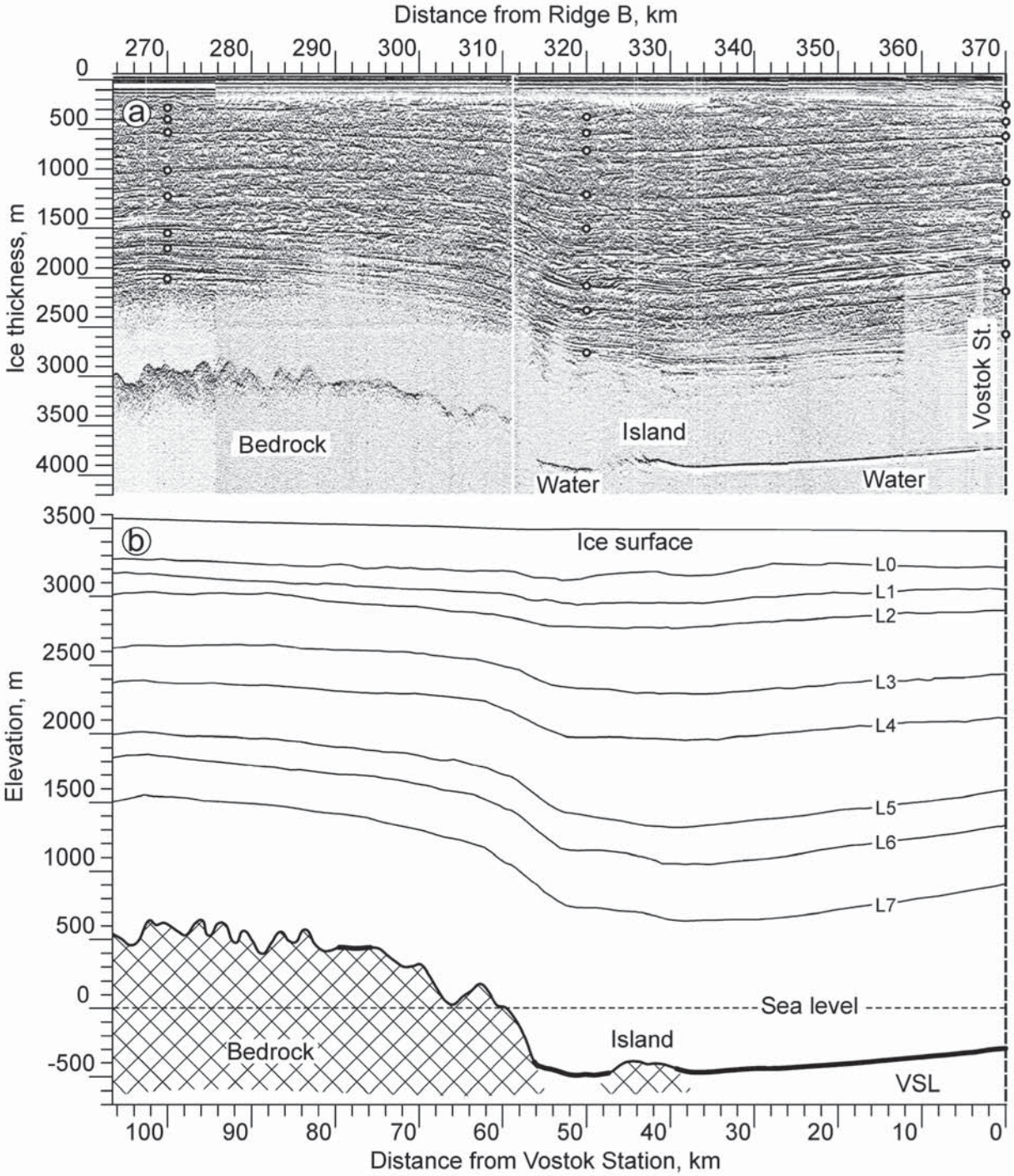

*Figure 6: Ground-based radio-echo time section (**a**) and the internal structure, surface and base topography (**b**) of the ice sheet over the 106-km distance along the ice flow line upstream of Vostok across Vostok subglacial lake (VSL). Reflection layers marked by open circles and numbered from L0 to L7 are used in this study for model constraining.*

[129]. It has been combined with the detailed geophysical observations around the lake provided by PMGE [67, 83, 84]. The re-examined Vostok flow line (VFL) and the flow tube confined between two neighboring flow lines are drawn in Fig. 4 perpendicular to the elevation contours for the grounded part of the ice sheet and follow the ice velocity field over the lake as determined in [5, 129] and recently confirmed by [138]. We introduce the longitudinal coordinate s as a distance measured from Ridge B along VFL with Vostok Station located at $s_0 = 370$ km.

Since the international BEDMAP project [65], many radio-echo sounding and seismic studies have been performed in Antarctica, in particular in the Lake Vostok area (e.g. [67, 83, 84, 125, 127]). The revised fragment of the general bedrock elevation map presented in Fig. 5 is a result of the newly launched ABRIS (Antarctic Bed Relief and Ice Sheet) project

[82]. The map is created by the Inverse Distance Algorithm with the 5×5 km grid at the 80-km averaging radius. The estimated accuracy (~ 200 m) is still limited substantially due to non-uniform distribution of the available RES profiles. The basic SPRI/NSF routes [20, 98] are shown in Fig. 5 by dotted lines. Some of these airborne radar transects were analyzed in [52, 117, 118]. Importantly, one of the flights, starting from Vostok Station (see Figs. 4 and 5), past closely to VFL in its middle part, 100-200 km upstream of Vostok.

The airborne and ground-based radar observations also provide valuable information on internal ice sheet structure (layering) controlled by the bedrock topography and environmental ice-flow conditions. A 106-km RES traverse was undertaken during the two field seasons of the 50 and 51-th Russian Antarctic Expeditions (2004-2006) on snow tractors by PMGE explorers over the subglacial lake area directly along VFL. The stacked radio-echo time section is depicted in Fig. 6a. Together with the underlying rock relief and the ice-water interface, eight isochronous reflection layers marked by open circles can be reliably discerned in the RES record. The layers are numbered downward from L0 to L7. Their altitudes, the ice sheet surface and base topography are plotted in Fig. 6b. These digitized data are used below for model constraining and validation. The western side of the lake, where the grounded ice meets the water, is clearly seen at a distance of $s_l \approx 315$ km from the ice divide, about 55 km from Vostok. Further, the ice, moving along VFL, passes over an island and touches the rocks between the grounding and floating points $s_g \approx 323$ and $s_f \approx 331$ km, respectively.

4.2 Ice flow description

The interaction of the ice sheet dynamics with heat transfer processes plays a special role in the vicinities of VFL passing through the vast subglacial lake. Taking account of these peculiarities, the joint problem of ice core age dating and paleoclimate reconstruction was considered in [130, 131] in the framework of the 2-D description of ice sheet movement along a fixed flow tube [86, 91]. The ice flow characteristics and the equation of convective heat transfer were presented in the boundary layer (shallow ice) approximation [31, 86, 87, 99] extended to the snow/firn compressibility effects [100] in a simplified form after [101, 107]. However, an important mass-conservation impact on vertical velocities near the western shoreline of the lake at the transition from the grounded to floating ice sheet flow pattern was neglected. Here we improve the velocity field description, using the original expressions derived in [100].

The principal assumption is made that the pattern of the spatial distribution of the ice mass balance b on the glacier surface does not change significantly with time t and the direction of ice motion is mainly determined by the bedrock relief. As a consequence, ice flow lines remain invariable, and the configuration of the fixed reference Vostok flow tube is characterized by its normalized width $H(s)$ and current ice-equivalent

Table 2. VFL model parameters

Parameter	Denotation	Value
Snow-firn densification		
Density of pure ice, kg m^{-3}	ρ_0	920
Surface-snow porosity	c_s	0.69
Exponential densification factor, m^{-1}	γ_s	0.021
Ice flow model		
Present-day accumulation rate at Vostok, cm yr^{-1}	b_0	2.15
Mass-balance exponential factor, °C^{-1}	η_b	0.11
Flow line length, km	s_0	370
Open lake area, km	s_f	331
Ridge-B highland boundary†, km	s_h	310
Glen flow-law exponent	α	3.0
Modified Glen flow-law exponent†	β	6
Shear-flow-rate factor	σ	$1,\ 0 < s < s_h$ $1 \to 0,\ s_h < s < s_f$ $0,\ s_f < s < s_0$
Surface-elevation slope factor†, MPa$^{\alpha}$ yr	ν	0.064
Model of ice-sheet thickness variations [110]		
Spatial mass balance amplification factor	γ_b	0.56
Ice-sheet growth feed-back factor	γ_l	2.5
Mean mass-balance excess†	e_b	0.44
Heat transfer model		
Specific heat capacity of ice, kJ (kg °C)$^{-1}$	$c(T)$	$c_0\left[1+\alpha_c(T+30)\right]$, $c_0 = 1.89$ $\alpha_c = 0.0037$ C^{-1}
Thermal conductivity of ice, W (m °C)$^{-1}$	$\lambda(T)$	$\lambda_0\left[1-\alpha_\lambda(T+30)\right]$, $\lambda_0 = 2.55$, $\alpha_\lambda = 0.0039$ C^{-1}
Surface heat transfer coefficient, m	χ	200
Latent heat of ice fusion, kJ kg^{-1}	L_f	333
Fusion temperature at the ice-lake interface†, °C	T_f	-2.7
Pressure depression coefficient†, °C MPa^{-1}	κ_p	0.081
Geothermal flux†, W m^{-2}	q_0	0.054
Thermal conductivity of rocks, W (m °C)$^{-1}$	λ_b	3.6
Thermal diffusivity of rocks, m^2 s^{-1}	a_b	$1.2 \cdot 10^{-6}$
Present-day ice surface temperature†, °C	T_{s0}	-58.5
Present-day inversion temperature, °C^{-1}	T_{i0}	-38.1
Geophysical metronome amplitudes, °C [3]:	A_1 (B_1)	6.28 (-2.81)
	A_2 (B_2)	5.31 (-1.86)
	A_3 (B_3)	-4.92 (2.35)
	A_4 (B_4)	-1.64 (-3.14)

† Parameters are constrained by available data and validated in computational experiments

thickness $\Delta(s, t)$. It is also relevant to define the vertical coordinate ζ as the relative distance from the glacier base expressed in terms of the equivalent thickness of pure ice and normalized by Δ.

The snow/firn and bubbly ice density ρ versus depth h can be presented [103, 107] as

$$\rho = \rho_0\left(1 - c_s e^{-\gamma_s h}\right),$$

where ρ_0 is the density of pure ice (constant value), c_s is the porosity of the surface snow and γ_s is the densification exponent factor. This directly yields a relationship between ζ and h

$$\zeta = 1 - \frac{h}{\Delta} + \frac{c_s}{\gamma_s \Delta}\left(1 - e^{-\gamma_s h}\right). \qquad (7)$$

The exponential approximation of the density-depth profile (c_s and γ_s in Eq. (7)) was deduced from the Vostok ice core measurements [57] and additionally confirmed in [24]. Ice properties and other model parameters used in our study are gathered in Table 2.

In terms of the above denotations, ice particle trajectories are the solutions of the following ordinary differential equations

$$\frac{ds}{dt} = u(s,\zeta,t), \qquad \frac{d\zeta}{dt} = \frac{\overline{w}(s,\zeta,t)}{\Delta(s,t)}, \qquad (8)$$

where u is the longitudinal velocity and $\overline{w}$ is the apparent vertical velocity in the (s, ζ)-coordinate system. The velocity field is given explicitly in [100]

$$u = \frac{A}{\Delta}\left[1 - \sigma\left(1 - \frac{\beta+2}{\beta+1}\left(1 - (1-\zeta)^{\beta+1}\right)\right)\right],$$

$$\overline{w} = -b + (1-\zeta)\left[b + w_0 + \frac{1-(1-\zeta)^{\beta+1}}{(\beta+1)H}\frac{\partial}{\partial s}(HA\sigma)\right]. \qquad (9)$$

Here $A(s, t)$ is the total ice flow rate along the reference flow line through the flow tube of a unit width

$$A = \frac{1}{H(s)}\int_0^s\left(b + w_0 - \frac{\partial\Delta}{\partial t}\right)Hds$$

and $w_0(s, t)$ is the ice accretion (melting) rate at the ice-water (rock) interface. By definition, σ is the proportion of the total ice flow rate through the flow tube due to plastic (shear) deformation of the glacier body ($0 \le \sigma \le 1$), and β is the modified Glen flow law exponent, which additionally takes into account the vertical temperature gradient [61]. Three regions are distinguished along the Vostok flow line: highland area $0 < s < s_h$ of the grounded ice sheet without sliding ($\sigma = 1$) at the bed ($s_h < s_l$), open lake area $s_f < s < s_0$ with the zero shear ($\sigma = 0$) at the glacier bottom, and the intermediate transition zone $s_h < s < s_f$ covering the vicinity of the western shoreline before the grounding line, the inlet, and the island (see Fig. 6). We assume that the σ parameter cosine-like monotonically decreases from 1 to 0 with distance s increasing from s_h to s_f where the ice sheet gets afloat. Both values β and s_h are considered as tuning parameters (see Table 2).

The ice sheet thickness is presented as

$$\Delta(s, t) = \Delta_0(s) + \delta\Delta(t), \qquad (10)$$

where $\Delta_0(s)$ is the present-day glacier thickness (in ice equivalent) along the flow line. Temporal ice sheet thickness fluctuations $\delta\Delta(t)$ are reconstructed after [101, 110]. This simplified multi-scale model for $\delta\Delta$ was verified, and its tuning parameters γ_b and γ_l given in Table 2 were constrained on the basis of the 2-D thermo-mechanically coupled model of Antarctic ice sheet dynamics [95]. Eq. (10) was later supported by 3-D simulations [96]. Another model parameter e_b in Table 2 is the relative ice-mass balance excess averaged over the area of the flow tube. It is directly calculated on the basis of the spatial distribution of ice accumulation rate.

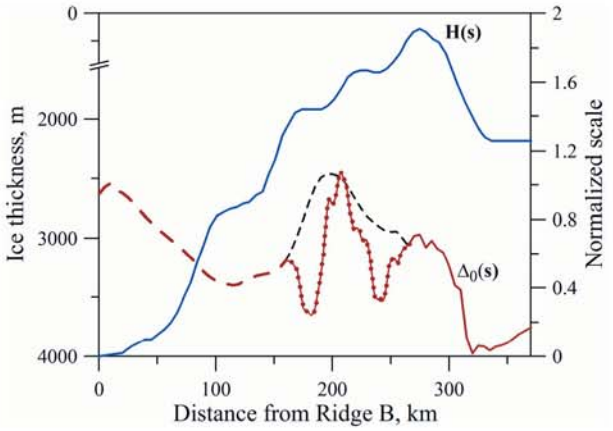

Figure 7: The normalized ice flow tube width H(s) vs. distance from Ridge B and the stacked present-day profile of the ice thickness $\Delta_0(s)$ along VFL (Fig. 4) in equivalent of pure ice with two possible versions of the intermediate part (see text).

The boundary between the glacial and refrozen ice (accreted ice thickness Δ_a) along the reference flow line over the lake is simultaneously determined from the accreted ice mass balance equation:

$$\frac{\partial\Delta_a}{\partial t} + \frac{1}{H}\frac{\partial}{\partial s}\left(H\Delta\int_0^{\Delta_a/\Delta} u d\zeta\right) = w_0. \qquad (11)$$

The present-day geometry of the ice flow tube is needed to employ the model (7)-(11). The relative flow tube width $H(s)$ versus distance s to Ridge B directly taken from Fig. 4 and available information on the ice sheet thickness $\Delta_0(s)$ (bedrock depth) in equivalent of pure ice

along VFL are plotted in Fig. 7. Based on the wide-angle reflection technique, the ice thickness at Vostok has been slightly re-estimated as 3775±15 m in [85], being also in agreement with other observational data. This is not far (within the 20-meter uncertainty of RES measurements) from the previously deduced value of 3755 m [64, 66] which is still used here for consistency with our earlier studies and transforms to 3722 m of the ice equivalent thickness under Vostok Station in Fig. 7. The most accurate 106-km profile of the glacier bottom upstream of Vostok (solid red line) is the 5-km running average of the RES data from Fig. 6b. The rest dashed (black and red) part of the bedrock relief corresponds to the residual cartographic data from Figs. 4 and 5 smoothed in 30-km scale. The intermediate red-dotted-line fragment overlapping the dashed black profile is the detailed 10-km running average of the bedrock relief from the airborne radar transect [117, 118] along the 100-km part of the SPRI/NSF RES route [19, 98] passing closely to VFL (see Fig. 4). The red (solid, dotted and dashed) stack presented in Fig. 7 is used further as the most reliable available description of the ice sheet base relief over VFL.

4.3 Heat transfer equation

A general equation of convective heat transfer in an ice sheet in the shallow-ice approximation [31, 87] combined with the ice flow line description [86, 91] in the (s, ζ)-coordinate system takes the form [100, 107]:

$$\rho_0 c\Delta^2\left(\frac{\partial T}{\partial t}+u\frac{\partial T}{\partial s}+\frac{\overline{w}}{\Delta}\frac{\partial T}{\partial \zeta}\right)=\frac{\partial}{\partial \zeta}\left(\lambda\frac{\partial T}{\partial \zeta}\right)+\overline{Q}\ , \qquad (12)$$
$$-t_0<t<0,\quad 0<s<s_0,\quad 0<\zeta<1.$$

Here $T(s, \zeta, t)$ is the ice temperature, $c(T)$, and $\lambda(T)$ are the specific heat capacity, and thermal conductivity of pure ice, respectively, and $\overline{Q}$ is the reduced strain heating. As in Eqs. (5) and (6), the time t is counted from the past, $t = 0$ corresponds to the present moment, and t_0 is an initial far moment before present (BP). Thermophysical characteristics of pure ice (see Table 2) are taken from [8, 33, 121].

In shallow-ice approximation with the use of Eqs. (9), the source of strain heating is written as [101]

$$\overline{Q}=g\rho_0\Delta\left|\frac{\partial l}{\partial s}\right|(\beta+2)\,A\,(1-\zeta)^{\beta+1}\ ,$$

where the ice-sheet surface slope along the flow line $|\partial l/\partial s|$ over the grounded part of the glacier is [130]

$$\left|\frac{\partial l}{\partial s}\right|=\frac{1}{g\rho_0\Delta}\left(\frac{\nu|A|}{\Delta^2}\right)^{\frac{1}{\alpha}}$$

and g is the gravity acceleration, α is the original Glen creep exponent in the ice flow law. A scaling parameter ν is proportional to non-linear ice viscosity. Its value given in Table 2 is fitted to the observed increase in the ice sheet surface elevation upstream from Lake Vostok to Ridge B (~290 m, see Fig. 4); the zero slope ($\overline{Q}=0$) is assumed over the deep water area $s_f < s < s_0$.

4.4 Boundary conditions

To complete the ice flow and heat transfer problem (7)-(12), boundary conditions should be imposed on the free ice-sheet surface and at the glacier bottom. Originally, Eq. (12) does not account for enhanced thermal resistance of snow and firn deposits in a relatively thin near-surface stratum of the ice sheet. As discussed in [107], a special heat balance equation should be formulated at the surface in this case to preserve the heat flow and to link it with the surface temperature T_s

$$-\frac{\chi}{\Delta}\frac{\partial T}{\partial \zeta}_{|\,\zeta=1}=T_{|\,\zeta=1}-T_s\ , \qquad (13)$$

where χ is the effective heat transfer coefficient expressed via relative density and thermal conductivity of snow and firn. Parameter χ was estimated for Vostok area in [101] on the basis of observational data [126, 136]. Its value, given in Table 2, was later validated on the new field measurements [111] confirmed in [29].

Long-term paleoclimatic temperature variations penetrate through the ice sheet thickness into the underlying rocks, and a conjugated boundary value problem should be formulated to describe the thermal state of the glacier at the ice-rock interface [93]. Preliminary computational experiments [130] show that, for realistic estimates of the geothermal flux q_0 in Antarctica [116], the grounded part of the ice sheet upstream of Vostok is frozen to the bed ($w_0 = 0$). Consequently, it is convenient to apply the integral Laplace transform and the Duhamel theorem of operational methods [9] to the heat conduction equation in the rocks and express the heat flux at the glacier bottom as a convolution integral

$$-\frac{\lambda}{\Delta}\frac{\partial T}{\partial \zeta}_{|\,\zeta=0}=q_0-\frac{\lambda_b}{\sqrt{\pi a_b}}\frac{\partial}{\partial t}\int_{-t_0}^{t}\frac{[T(s,\zeta=0,\tau)-T(s,\zeta=0,t=-t_0)]\,d\tau}{\sqrt{t-\tau}} \qquad (14)$$
$$0<s<s_l\ ,$$

Here a_b, λ_b are the thermal diffusivity and conductivity of the rocks [73, 95]. Linear vertical temperature distribution, consistent with the geothermal flux q_0 and surface temperature T_s, is set as an initial temperature field at a time $t = -t_0$ far in the past.

Over the lake, $s_l < s < s_0$, the glacier base is at the melting point,

$$T_{|\,\zeta=0}=T_f\ ,\quad s_l<s<s_0\ , \qquad (15)$$

with the ice fusion temperature T_f linearly related to pressure p

$$T_f = T_{f0} - \kappa_p p \ .$$

The fusion temperature at zero pressure T_{f0} and pressure depression coefficient κ_p depend on the lake water salinity and the concentration of dissolved air (gases) [54]. Their values resulting in T_f most consistent with the borehole temperature measurements at Vostok are given in Table 2.

The accretion ice at the contact of the ice sheet with the lake water is generally formed of the local water frozen due to the upward heat flux (cooling) though the glacier body but, in principle, we do not exclude a possibility that a certain amount of frazil ice [76, 77] can be brought by ascending fresh water flow from the colder northern ice-melting area [117, 125]:

$$w_0 = w_f - \frac{1}{\rho_0 L_f} \frac{\lambda}{\Delta} \frac{\partial T}{\partial \zeta}_{|\zeta=0} \ , \qquad (16)$$

where w_f is the rate of frazil formation and L_f is the latent heat of ice fusion. The accretion rate w_0 is assumed to be zero over the island.

4.5 General algorithm and strategy of computations

The age t_d of an ice particle at a depth of h_d related to the ζ_d level by Eq. (7) under Vostok Station at $s = s_0$, that is the ice core time scale, is determined from equation $\zeta(-t_d) = 1$, where the ice particle trajectory $(\zeta(t), s(t))$ is the backward-in-time solution of Eqs. (8)-(10) at the initial conditions $s(0) = s_0$, $\zeta(0) = \zeta_d$. Correspondingly, the deposition site of the particle is $s_d = s(-t_d)$.

Implicit finite-difference schemes were used to solve the differential equations (11) and (12) at the boundary conditions (13)-(16). "Left-angle" first-order approximations along the s-axis provide stability of the computational algorithm based on the sweep method along the ζ-axis.

The climatic input of the model over the recent 420-kyr history covered by the Vostok deuterium record [78] is represented by Eqs. (2), (3), and (6) and the iteratively calculated glaciological time scale. For earlier times, the scaled geophysical metronome (5) is employed to extrapolate the inversion temperature variations in Eqs. (3) and (6) into the past.

An interactive computer system was developed to perform necessary numerical experiments in order to constrain the improved thermo-mechanical ice flow line model and its climatic input by available geophysical and glaciological data. Our previous studies [101, 112, 130, 131] show that the simulated features of the ice-flow and temperature fields in the ice sheet are selectively sensitive to different model uncertainties. Thus, the general strategy of the ice core data interpretation was in sequential and iterative fitting the model to various independent sets of observational data (borehole temperature measurements, accumulation rates deduced form air bubble properties, ice age markers, isochronous reflection layers, and other sources of glaciological information) to come to the most consistent (best-fit) model predictions and, consequently, to more reliable paleoclimatic reconstruction and ice core age dating. The following general guide lines were used in our complex optimization procedure.

1. A sufficient set of age markers statistically independent and uniformly distributed versus depth at a certain site under consideration ($s = s_0$) reliably constrains the ice-volume flow rate $A(s = s_0, t)$ through the prescribed reference flow tube in Eqs. (9). For a given present-day accumulation b_0 at Vostok, the flow rate determines the isotope/temperature slope C_T in the precipitation model (2) and (3) and allows tuning the shape of the spatial profile $\bar{b}(s)$ to deduce the best-fit ice age-depth relationship.

2. Although limited in distance, the isochronous reflection layers (see Fig. 6), especially in the upper, near-surface part of the ice sheet, also deliver unique information on the $\bar{b}(s)$ -distribution along the flow line. The local configuration and the total descent of isochrones in the deeper part of the glacier within the transition zone $s_h < s < s_f$ at the western side of the lake are mainly controlled by the modified Glen exponent β and the boundary coordinate s_h.

3. The temperature gradient in the deeper part of the ice sheet above the lake remembers the thermal state of the bedrock and the geothermal flux q_0 over the highland area in Eq. (14) and determines the ice accretion rate w_0. Through Eq. (11), the ice flow rate (the travel time across the lake) and the accretion rate control the lake-ice thickness Δ_a which, being measured at Vostok [44], delivers the information on q_0. As discussed in section 2, the borehole thermometry constrains the C_i-coefficient (the product $C_i C_T$), the scaling factor α_p, and the present-day surface temperature T_{s0} in Eqs. (6) after substitution of Eq. (2). The observed temperature profile extrapolated to the ice sheet bottom provides an estimate for the fusion temperature T_f and the κ_p-coefficient in Eq. (15).

4. Finally, the reconstructed past temperatures on the ice sheet surface and the air bubble number density measured in the upper part of the Vostok ice core can be recalculated [55, 56, 58] into local LGM-Holocene variations of the accumulation rate to determine (and/or validate) directly the temporal slope C_T in Eqs. (2) and (3). The rest (deeper part) of the available bubble number concentration profile represents the spatial distribution of the accumulation rate $\bar{b}(s)$ upstream of Vostok.

Numerous series of hundreds of computational experiments took totally about two years of systematic iterative tests and data analyses. The inferred model parameters are presented in Tables 1 and 2, and the obtained results are discussed below, in the final section.

5. Results of model constraining and ice core data interpretation

5.1 Revised glaciological time scale

The studies of ice sheet dynamics along the Vostok ice flow line and ice age predictions reviewed in section 3 were based on simplified models and suffered from the lack of accurate geographic data. Furthermore, invariable spatial distribution of the accreted ice thickness was implicitly assumed at the glacier bottom over the lake in [112]. However, the total amount of refrozen ice is directly linked to the local velocity of the ice sheet motion and both characteristics undergo paleoclimatic fluctuations. These perturb strain rates in the glacier body floating across the lake and, as a consequence, affect the ice age-depth relationship. Preliminary series of computational experiments performed in [130, 131] showed that imperfectness of the model and existing uncertainties in its environmental input can lead to high local errors in ice age predictions within the estimated standard deviations of ±3.6 kyr [112]. Here we use the improved 2-D ice flow line model (7)-(16) with the general description of the velocity field transition from the grounded to floating ice sheet flow pattern, ice accretion at the glacier bottom over the lake, and the re-examined geographic data (Figs. 4 and 5) based on the recent cartographic materials and RES profiling (Fig. 6) along VFL.

Special attention is paid to better constrain the spatial distribution and temporal variations of the ice mass balance given by Eqs. (2) and (3). Available data are gathered in Fig. 8. The present-day ice accumulation rate at Vostok is assumed to be $b_0 = 2.15$ cm yr^{-1} which is close to the 190-year mean value [24] and provided the best-guess time scale GTS-II for Vostok ice core [112]. The air bubble number density profile measured at Vostok confirmed [56] the best-fit isotope/inversion temperature slope $C_T = 6.1$ ‰°C^{-1} deduced at $\gamma_m \approx 4.6$ in [130, 131] with the use of the GMTS age markers and allowed reconstruction of the accumulation rate profile $\bar{b}(s)$ over ~50 km across the lake (Fig. 8, curve 1). The latter result is in agreement with the field studies by Popov and others [81, 84]. On average, the 30-35% increase in the accumulation rate at the western side of the lake is also supported by the isotopic and stratigraphic studies in pits (personal communication by A.A. Ekaykin). These estimates give at least 30% higher present-day b-values at 35 and 59-km distance and a 40% increase at 96 km from Vostok (Fig. 8, squares). The mean accumulation rate over the recent 190 years (2.25±0.04 cm yr^{-1}) has been directly calculated from the depth of the Tambora eruption layer observed in the pit at the end of the VFL radar route, 106 km upstream of Vostok (Fig. 8, diamond), and practically coincides with that at Vostok. The ice mass balance enhancement factor of 1.65 estimated in [40] for Ridge B at the location of the Dome B ice core (DB site in Figs. 4 and 5) corresponds to the triangle in Fig. 8. The normalized spatial distribution of the accumulation rate deduced in [52] form the air-borne radar observations along the flight route approximately parallel to VFL and passing 40-50 km northward is also shown as curve 2. All these data considerably reduce the $\bar{b}(s)$ -profile uncertainty.

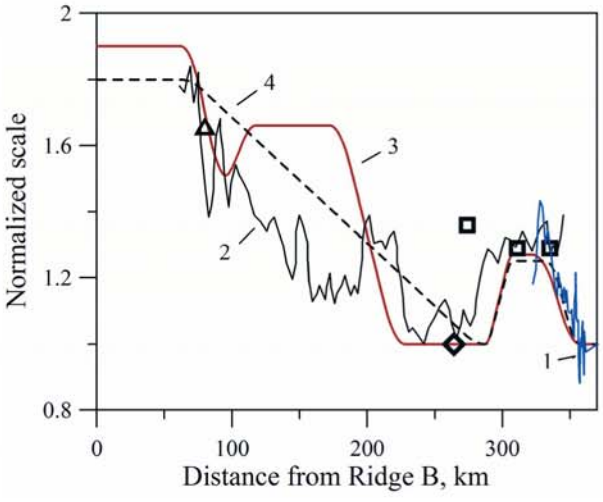

Figure 8: The normalized accumulation rate $\bar{b}(s)$ vs. distance from Ridge B along VFL (Fig. 4) deduced from air bubble number density [56] (curve 1) and RES data [52] (curve 2); the best-fit spatial profiles (curves 3 and 4) correspond to different versions of the bedrock relief in Fig. 7. Available field observations are shown by symbols: squares - isotopic and stratigraphic studies in pits (pers. com. by Ekaykin), diamond - the depth of the Tambora eruption layer, triangle - the estimate [40] for the DB site in Figs. 4 and 5.

To find the best-guess environmental conditions and tune the ice sheet flow model, we used eight RES reflection (isochronous) layers L0-L7 depicted in Fig. 6b and a selected set of the most reliable age markers. In accordance with our previous analysis [112] illustrated by Fig. 3, the less accurate DH control points were excluded from consideration. It is also clear that the 39 GMTS age-depth correlation points practically cover most of the 8 age markers from [74, 75] except for the universal ^{10}Be peak [88, 142] observed in the Vostok ice core around the 601-meter depth and reliably dated as 41±2 kyr. Thus, the employed set of age control points was composed of the latter beryllium event and 34 GMTS ice age markers older 50 kyr from [3].

The first series of computations were performed with the detailed 106-km RES profile of the ice-sheet base (Fig. 6b) continued by the large-scale smoothed bedrock relief (Fig. 7, black and red dashed line) from the topographic map in Fig. 5. The simple spatial distribution of the normalized accumulation rate $\bar{b}(s)$ drawn by the black dashed line in Fig. 8 in accordance with the presented observational data was found to be in agreement with the near-surface RES reflection layers L0-L2 in Fig. 6b and delivered the best-fit ice age-depth relationship. However, the standard deviation (SD) of

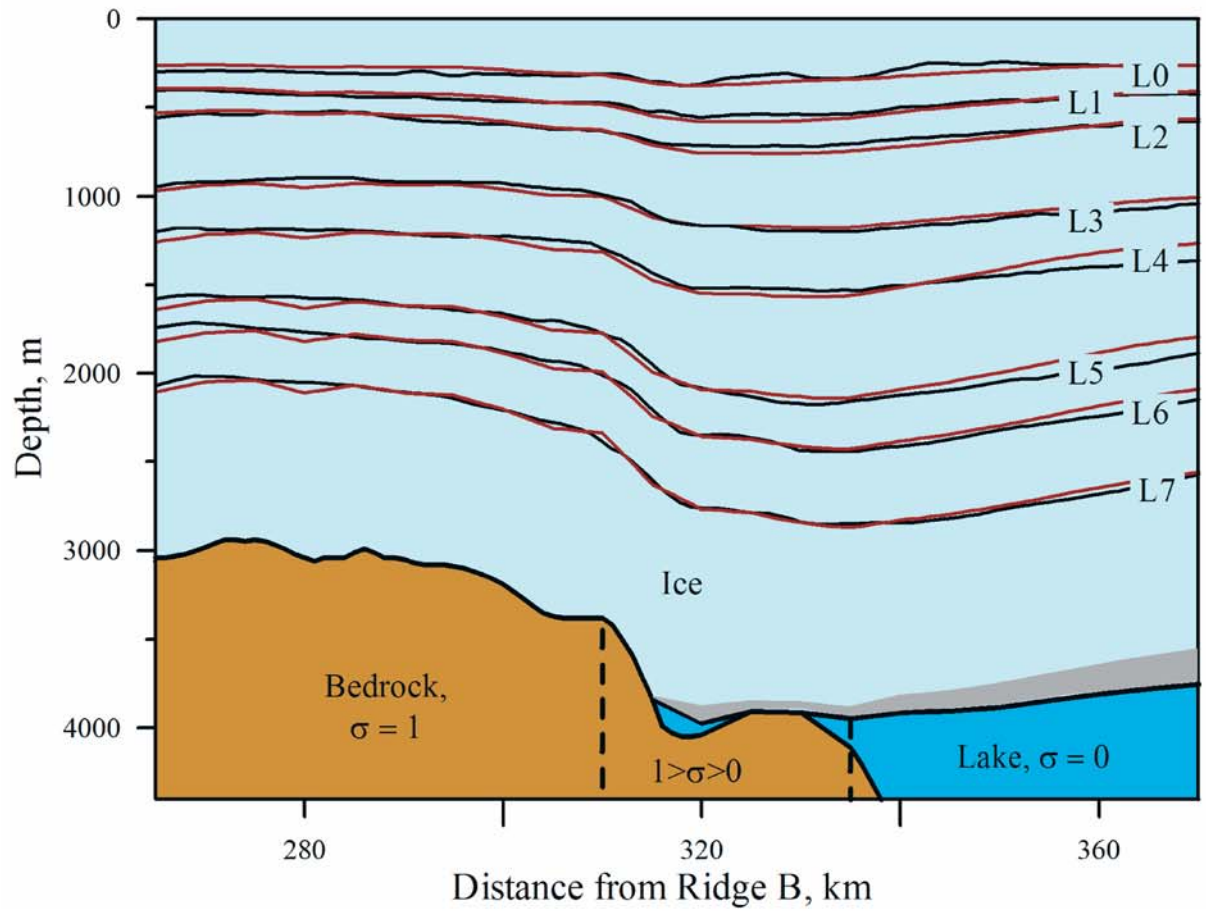

Figure 9: Comparison of the best-fit simulated isochrones (red lines) dated 11.2, 23, 37.5, 73, 94.7, 126, 150, and 210 kyr with the respective reflection layers L0 to L7 (black lines) from Fig. 6b. Accreted ice layer is shaded.

the simulated deeper isochrones from the RES reflection layers L3-L7 (Fig. 6b) reached 6-8 kyr. The calculated timescale deviated from the selected age markers by5.0-5.5 kyr, exceeding considerably the GMTS approximation level of ~4.5 kyr by GTS-II achieved in [112]. More sophisticated geographic profiles of the accumulation did not improve the convergence of the modelled ice ages to the selected control points.

Much better results were obtained when the intermediate part of the bedrock elevation profile was detailed by the airborne radar record [117, 118] along the adjacent route [20, 98] as shown in Fig. 7 (red-dotted line). Fig. 9 demonstrates a good agreement between the simulated and observed isochrones achieved in this case at age SD of 1.3, 2, 2.1, 2.5 2.9, 2.2, 5.4, and 3.8 kyr for the layers L0 to L7, respectively. The depth deviations are 31, 20, 23, 28, 45, 46, 36, and 24 m, being comparable on average with errors of RES data interpretation [85]. Correspondingly, the best-fit model parameters $\beta = 6$ and $s_h = 310$ km were deduced.

Computational experiments show that isochrones near Vostok, within the 106-km PMGE radio-echo sounding section in Figs. 6 and 9, are not noticeably sensitive to short-scale spatial variations of the accumulation rate in the upstream VFL area within a 270-km distance from the ice divide. Accordingly, this part of the $\bar{b}(s)$ -profile was adjusted to reduce SD between the modelled (glaciological) time scale and the ice-age markers at Vostok. For the detailed stacked bedrock relief (Fig. 7, red line), we succeeded to reach the expected SD minimum of 4.4 kyr with the accumulation rate distribution plotted in Fig. 8 by the red solid line. The total ice flow rate $A(s = s_0, t)$ through the flow tube was validated on the present-day surface ice velocity of 2.00±0.01 m yr^{-1} measured at Vostok by Wendt and others [138] and obtained in the simulations around 2.03 m yr^{-1}. For a given geothermal flux q_0, the ice flow could also be verified through the accreted ice thickness at Vostok.

The best-fit ice age-depth relationship is presented in Fig. 10a together with the used control points. This glaciological time scale, designated after [131] as GTS-III, summarizes the earlier efforts to improve the Vostok ice core age dating on the basis of ice flow line modeling. Different glaciological time scales are compared in Fig. 10b. The respective standard deviations of GTS-III from the average time scale and GTS-II developed in [112] are 2.7 and 3.0 kyr, being in full agreement with their estimated quality (2.2 and 3.6 kyr). SD between the newly simulated time scale GTS-III and GTS-I proposed in [75] is 3.5 kyr and

remains within the ±3-3.5-kyr deviation limits related, as discussed in [131], to uncertainties in the paleoclimatic and geographic conditions and differences in the employed thermo-mechanical models. GTS-I deviates from the 35 age markers used in our study by 5.0 kyr on average (comp. with the 4.4-kyr SD of GTS-III). At the same time, GTS-I and GTS-III have comparable statistical validity characterized by the mean variances of 2.3 and 2.8 kyr with respect to the eight age markers used in [75]. From this point of view, GTS-III based on a substantially improved modeling approach with more accurate and broader data scope may be considered as a further step towards developing a glaciological time scale for the Vostok ice core with the age errors on the order of 2 kyr or less on average down to a depth of 3310 m. The new ice age-depth relationship is presented in Table 3 together with the ice particle deposition sites given as distances from Vostok.

Necessity of the sophisticated modeling and importance of our knowledge about the environmental (paleoclimatic and geographic) conditions of the ice sheet flow for correct ice age predictions were discussed and demonstrated earlier in computational experiments [131]. Here to emphasize and illustrate this point, the preliminary best-fit time scale simulated for the roughly smoothed part of the bedrock (Fig. 7, black dashed line) and the simplified spatial distribution of the accumulation rate (Fig. 8, black dashed line) is also shown in Fig. 10b by the black dashed line. Corresponding changes in the ice age estimates around 120-170 kyr (~1600-2200 m depth interval) reach 10 kyr. Numerical tests show that this discrepancy is caused by the substantially lesser ice thickness around 170-190 and 230-250 km from the ice divide in the case of the smoothed bedrock profile. The systematic shifts between GTS-I, II and III timescales within 70-170 kyr period are also mainly due to differences in the bedrock topography and spatial distribution of the accumulation rate.

In spite of the ice flow disturbances observed in 3310-3330 m depth interval [78], recent studies of the deepest part of the Vostok glacier ice [120] showed that the glacial stages 14 and 16 are still discerned in the dust concentration record within the depth intervals 3380-3405 m and 3435-3450 m, respectively, and most likely the interglacial stage 17 covers the depth range from 3460 to 3470 m. This suggests that the ice, at least to a depth of 3470 m, has undergone only local perturbations [89]. Hence, an extension of the best-fit time scale GTS-III toward the boundary with the accreted lake ice, to a depth level of 3540 m [44], can provide a new better estimation of possible maximum variations of ice ages. The statistically expected age-depth distribution is given in Table 3 and plotted in the inset in Fig. 10a. For example, the ice age at the 3530 m depth, 10 m above the contact with accreted ice, could reach ~1000 kyr, provided that the basal ice flow had not been disturbed. The depth ranges of the stages 14, 16, and 17 suppositionally observed in the dust record

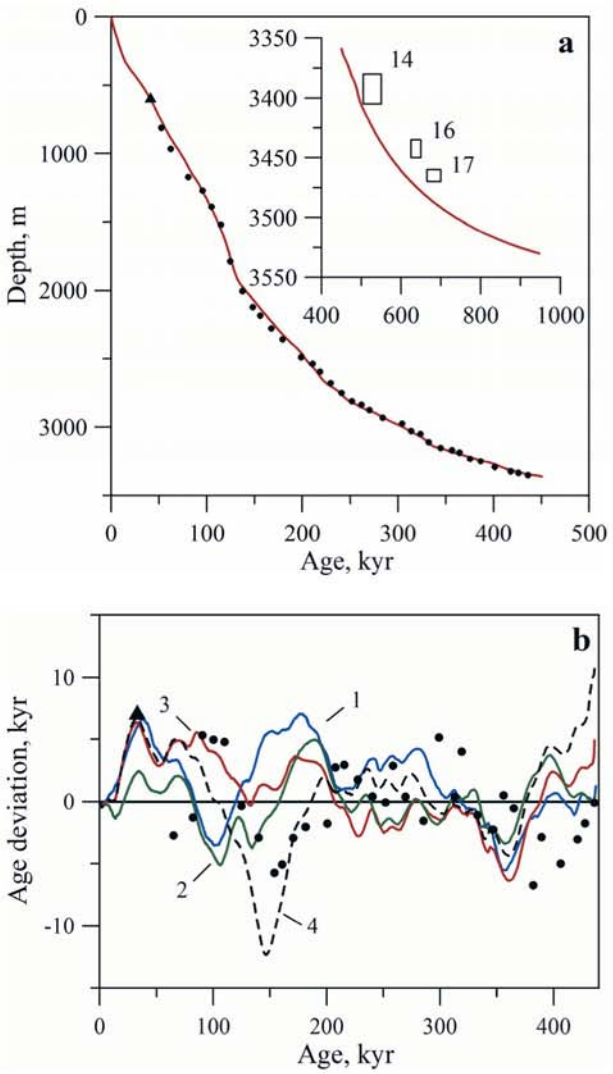

*Figure 10: Ice age dating at Vostok. **(a)** Best-fit glaciological time scale GTS-III (red line) compared to GMTS (filled circles) and beryllium-10 (triangle) age markers from [3, 88] used for constraining the ice flow model. The inset shows the extension of GTS-III to the 3530 m depth level, 10 m above the boundary with the accreted lake ice. Rectangles and numbers are the climatic stages discerned in the Vostok dust concentration record. **(b)** Deviations of the glaciological time scales GTS-I [75], GTS-II [112] and GTS-III (curves 1-3, respectively) from the average time scale for Vostok ice core [112] (zero line); curve 4 corresponds to the dashed fragment of the bedrock relief in Fig. 7, age markers are taken from **(a)**.*

[120] and their respective durations (505-550, 625-650, 665-700 kyr) estimated after [4] are marked by rectangles in the inset and indicate that the deeper part of GTS-III may underestimate ice ages by ~20-40 kyr. It should be emphasized here that the real basal ice deformation history is much more complicated than that modelled in our simulations and the time scale extension is given just to illustrate a possible tendency of the ice age growth with depth.

Table 3. Glaciological time scale GTS-III for Vostok ice core and ice particle deposition sites (distance from Vostok)

Depth m	Age kyr	Dep.site km	Depth m	Age kyr	Dep.site km	Depth m	Age kyr	Dep.site km
0	0	0	2198.0	164	222.1	3090.1	328	297.5
113.5	4	7.3	2229.6	168	224.9	3113.3	332	298.6
200.1	8	12.5	2261.7	172	227.7	3136.1	336	299.6
286.8	12	16.0	2294.1	176	230.5	3147.1	340	300.7
343.6	16	20.5	2325.0	180	233.3	3155.2	344	301.6
383.6	20	25.0	2353.5	184	236.2	3163.9	348	302.5
420.9	24	29.5	2380.7	188	239.2	3172.3	352	303.5
458.9	28	34.2	2407.9	192	242.4	3180.2	356	304.6
498.3	32	38.9	2436.7	196	245.6	3188.0	360	305.6
541.0	36	44.2	2468.6	200	248.6	3195.9	364	306.7
588.6	40	50.2	2506.0	204	251.3	3203.8	368	307.9
640.9	44	57.0	2540.6	208	254.1	3211.9	372	309.1
698.0	48	64.9	2571.7	212	256.7	3220.2	376	310.3
754.7	52	72.4	2607.5	216	258.7	3228.8	380	311.5
808.7	56	78.9	2645.4	220	260.5	3237.5	384	312.7
860.5	60	85.5	2673.9	224	262.3	3245.4	388	314.0
906.0	64	92.3	2694.6	228	264.0	3252.7	392	315.5
949.1	68	99.5	2712.7	232	265.8	3260.1	396	317.1
992.2	72	106.9	2730.9	236	267.7	3268.8	400	318.3
1037.5	76	114.2	2753.2	240	269.1	3279.3	404	320.4
1088.7	80	120.7	2782.7	244	270.3	3290.8	408	321.8
1140.4	84	126.9	2805.3	248	271.6	3301.8	412	323.0
1182.1	88	133.2	2820.1	252	272.8	3310.9	416	321.8
1226.2	92	139.4	2833.9	256	273.9	3318.1	420	324.2
1280.2	96	145.7	2849.1	260	274.9	3324.2	424	325.3
1334.0	100	152.1	2863.4	264	276.0	3330.8	428	326.4
1386.3	104	159.5	2875.4	268	277.1	3338.1	432	327.3
1444.7	108	168.3	2886.5	272	278.3	3344.2	436	327.3
1508.8	112	176.9	2898.0	276	279.6	3348.6	440	329.5
1575.8	116	184.0	2911.5	280	280.8			
1651.5	120	189.6	2927.2	284	282.0	**Extrapolated time scale**		
1743.6	124	193.8	2943.1	288	283.2	3360	448	330
1839.6	128	197.0	2957.3	292	284.4	3370	459	331
1918.1	132	200.1	2970.2	296	285.6	3390	485	336
1961.7	136	202.9	2982.8	300	286.9	3410	502	338
1995.0	140	205.7	2996.0	304	288.3	3430	532	342
2027.2	144	208.5	3010.5	308	289.6	3450	570	344
2061.0	148	211.3	3026.6	312	291.1	3470	618	348
2095.9	152	214.0	3041.9	316	292.6	3490	686	353
2130.9	156	216.6	3056.2	320	294.2	3510	776	358
2165.2	160	219.4	3071.7	324	295.9	3530	925	362

5.2 Paleoreconstructions

A simplified quasi-one-dimensional heat transfer model was used for temperature simulations in the vicinities of Vostok Station discussed in section 2. In particular, longitudinal heat convection was neglected in paleoclimatic borehole-temperature interpretations [3, 101, 104, 113]. However, significant geographic changes in ice accumulation rate, almost twofold increase in ice thickness (see Figs. 6-8), and considerable temperature contrast between the "cold" grounded and "warm" floating parts of the glacier along VFL result, as shown below, in large horizontal temperature gradients in the near-bottom ice stratum. The new series of computational experiments were started in [130, 131] on the basis of the 2-D flow line description of heat transfer processes in ice sheets to additionally constrain and/or validate the principal parameters T_{s0}, C_T, C_i, α_p of the climatic sub-model (2)

and (6). Here we continue these studies, using the improved thermo-mechanical model presented in section 4.

Following [130], paleotemperatures were deduced from the continuous temperature profile measured by R. Vostretsov in the record 3620 m deep borehole at Vostok. The preliminarily processed data [3] were shifted by 0.6°C to minimize the systematic error and to make the measurements consistent with the upper part of high-precision Rydvan's thermometry survey [106]. In accordance with [77, 122], the spatial temperature drop of 2.3°C from Ridge B to Vostok Station was introduced into Eq. (6) in T_{s0} after [131]. The present-day borehole temperature profile and mismatch between the measured and fitted temperatures are shown in Fig. 11a. SD is about ~0.03°C and compares to the accuracy of the data.

All constrained climatic parameters are given in Table 1. The present-day ice surface temperature $T_{s0} = -58.5$°C at Vostok is similar to that found in [101]. The deduced ice fusion temperature at the ice-sheet bottom, 3755 m below the surface, $T_f = -2.7$°C is in agreement with [54]. At the same time, the inferred estimates of $C_i = 0.79$ (the product $C_i C_T = 4.8$ ‰°C^{-1}) and $\alpha_p = 0.06$, being close to those of [130, 131], differ considerably from the previous studies [3, 101, 104, 113] based on the simplified models and less accurate or limited-in-depth borehole temperature measurements.

Another temperature profile was measured at Vostok by C. Rado (personal communication by J.R. Petit) at the end of 1997 down to 3420 m after 8-month break in drilling operations. Being in agreement with Rydvan's measurements in its upper part, this survey reveals 0.2-0.3°C colder ice with respect to the corrected Vostretsov's data in the deeper part of the borehole. As shown in [130], the best-fit fusion temperature in this case decreases accordingly with only minimum changes in scaling factors C_i and α_p at the same SD level. Thus, the isotope/temperature transfer function and the past accumulation rates given by Eqs. (2), (3) and (6) with the recommended parameters from Tables 1 and 2 can be considered as well established and reliably constrained.

The recovered surface and inversion temperature fluctuations are plotted in Fig. 11b. In agreement with [130, 131], the amplitudes of ΔT_s are noticeably less than before in case of the spatially one-dimensional heat transfer models [3, 101, 104, 113]. In particular, the Last Glacial Maximum (LGM) surface temperature at Vostok is found to be -67.8ºC for the non-zero surface temperature spatial gradient, that is only 11.4ºC lower than the Holocene-optimum temperature -56.5ºC. It was 12.5-14.0ºC lower in [130, 131] for the simplified ice flow description at the grounding line, while the transitions of 15-20ºC were deduced previously. Special computational tests confirm that the latter difference is caused by the considerable decrease in the ratio w/Δ in Eq. (12) along VFL neglected in the simplified descriptions as well as by the use of the more reliable

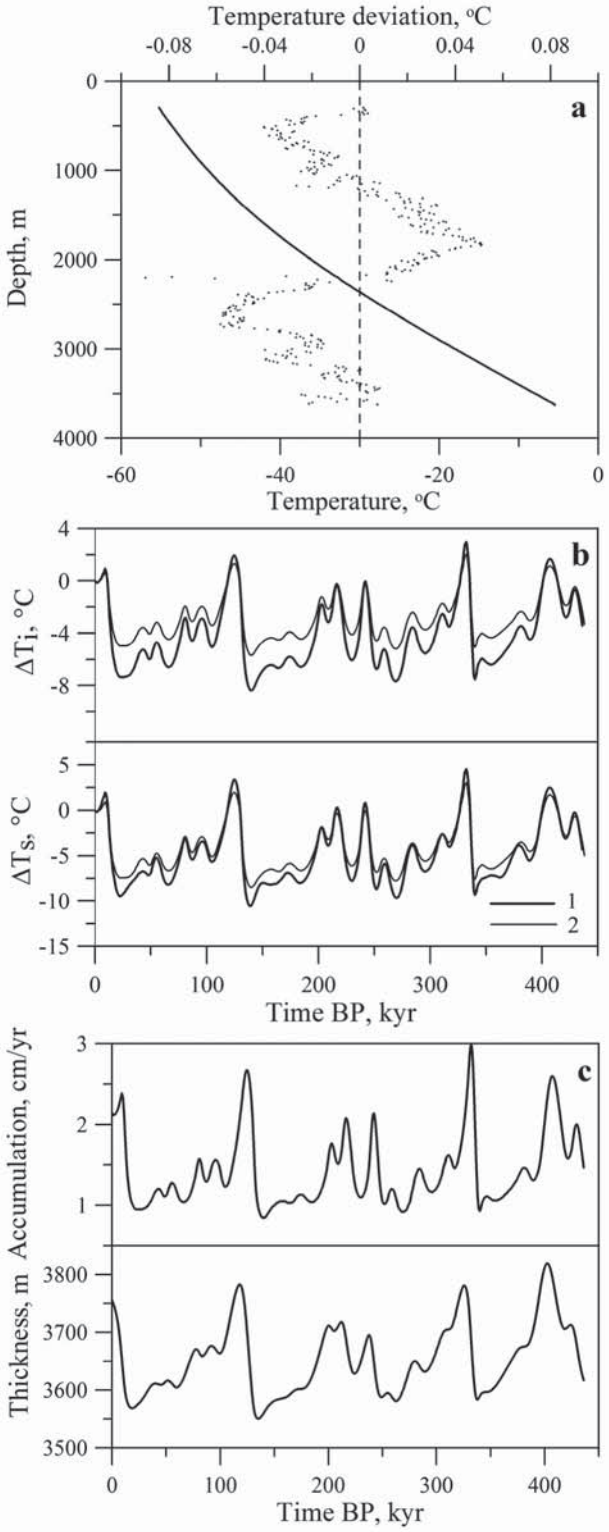

Figure 11: Paleoclimatic model constraining. ***(a)*** *The borehole temperature profile at Vostok and mismatch (dots) between the measured and calculated temperatures.* ***(b)*** *Past inversion and surface temperature variations from Eqs. (2) and (6) at the best-fit parameters $C_T = 6.1$ ‰°C^{-1}, $C_i = 0.79$, $\alpha_p = 0.06$ (curves 1) and from Eqs. (2) and (4) at geographic estimates $C_T = 9$ ‰°C^{-1} and $C_i = 0.67$ [41,42] (curves 2).* ***(c)*** *The reconstructed ice accumulation rate and ice thickness variations at Vostok.*

and complete thermometry data instead of the temperature stack [101, 113]. Earlier, the best fit between borehole temperature measurements and simulations was generally found at a higher accumulation rate $b_0 \sim 2.4$ cm yr^{-1} which corresponds to a 50-year mean value at Vostok [2, 24]. This, most likely, partly counterbalanced in one-dimensional approximation a considerable increase in accumulation rate upstream towards Ridge B.

The new estimate of the LGM-Holocene temperature increase is now substantially closer to the conventional predictions (~9ºC) based on geographic data, although remains about 25% higher, as might be expected from well understandable difference between the spatial and temporal isotope/temperature slopes [45]. Another interesting peculiarity is that the inferred inversion/surface temperature slope $C_i = 0.79$ is closer to unity than its geographic analogue $C_i = 0.67$ in [42] and predicts more commensurable amplitudes of temporal fluctuations of inversion and surface temperatures than the difference between their spatial variations (see Fig. 11b). These results are also consistent with the independent meteorological observations [21] (see Table 1, comp. Figs. 2b and 11b).

Accumulation rate variations determined by Eqs. (2) and (3) at the best-fit value of $C_T = 6.1$ ‰°C^{-1} with $\gamma_m = 4.6$ and the corresponding changes in the ice-sheet thickness at Vostok described by the simplified model [110] are presented in Fig. 11c.

Special computational experiments showed that the use of the more general equations (1) instead of Eq. (2) did not noticeably change the discussed above paleoclimatic reconstructions. The performed analysis confirms the inferred tuning parameters of the climatic sub-model (2), (3) and (6) (bold values in Table 1) as most reliable.

5.3 Simulated ice flow characteristics

The simulated contemporary distribution of the surface ice velocity along VFL is presented in Fig. 12a by solid line. Its spatial variation follows the changes in configuration of the ice flow tube, while the absolute values are determined by the current accumulation rates. For the 190-year averaged present-day accumulation rate ($b_0 = 2.15$ cm yr^{-1}) the calculated ice velocity at Vostok in Fig. 12a is about 2.03 m yr^{-1} and approaches 2.3 m yr^{-1} for the recent 50-year mean value ($b_0 = 2.4$ cm yr^{-1}). Both estimates are in perfect agreement with the direct observations 2.00±0.01 m yr^{-1} [138] and 3±0.8 m yr^{-1} [5]. The normalized spatial profile of the surface velocity remains practically (within 5%) constant in time [130]. Relative temporal variations of the surface velocity are shown in Fig. 12b. They are practically identical for different sites along the flow line and reveal two times lower velocities around 10 kyr BP after the LGM period.

Prediction of spatially non-uniform and variable-in-time ice flow rates upstream of Vostok Station (see Figs. 12a, b) is an important result of the computations which allows a more accurate estimation of the travel

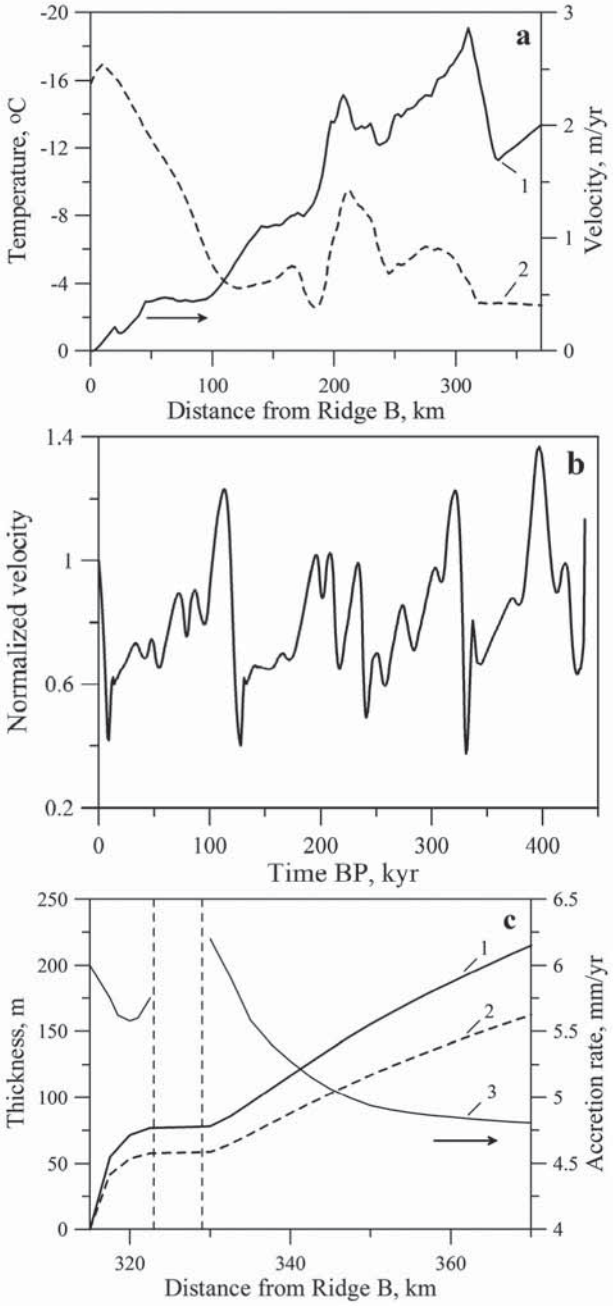

*Figure 12: Ice sheet dynamics and basal conditions along VFL. (**a**) The present-day surface velocity (curve 1) and temperature distribution at the glacier base (curve 2). (**b**) Normalized surface velocity variations in central Antarctica. (**c**) The present-day refrozen ice thickness (curve 1), a minimal accreted ice layer (curve 2) after interglacial periods and the distribution of the ice accretion rate over the lake (curve 3).*

time needed for ice to float across the lake. The transit time varies from its minimum of about 28 kyr to maximum of 41 kyr during interglacial and glacial periods, respectively. For example, due to essentially reduced velocities in the recent glacial period, it took about 10 kyr for the present-day Vostok ice to cross the 11 km-wide embayment near the western side of the

lake and, totally, 40 kyr to approach Vostok Station. This differs considerably from preliminary predictions discussed in [117] and from the respective values of 4 and 20 kyr found in [5] under the assumption of the constant ice velocity over the lake. The above estimates characterize the motion of the surface ice. Due to the basal drag in the embayment-island area (see Fig. 6b), the bottom ice journey is even longer and takes from 38 to 57 kyr.

Ice core studies at Vostok [44] revealed 215 m of refrozen lake ice at the glacier bottom provided that the total ice sheet thickness is 3755 m [64, 66]. At zero frazil formation rates ($w_f = 0$ in Eq. (16)), this constrains the geothermal heat flux as $q_0 \approx 0.054$ W m^{-2} with accuracy not worse than ±5% in agreement with the general estimates of [116] for central Antarctica. As before [130], the simulated present-day basal temperatures along the major part of the grounded ice flow line (see Fig. 12a) do not reach the melting point and remain systematically below -4°C. Consequently, only two factors control the ice accretion: (1) the thermal interaction of the cold glacier (overcooled with respect to the melting point) with the lake water and (2) the convective drift of the total geothermal heating from the lake floor to the northern half of the lake due to the water circulation (e.g. [117, 125]). Without direct geothermal heating from the lake, the heat losses through the ice thickness in the southern part are fully counterbalanced by the water freezing. Contemporary distribution of the accreted ice Δ_a and freezing rates w_0 along the VFL are shown in Fig. 12c by solid curves 1 and 3, respectively. In accordance with these computations, about 75 meters of the accreted ice are formed over the embayment near the western side of the lake at the maximum accretion rates of ~6-6.5 mm yr^{-1}. No water freezing is assumed on the island surface, and the mean accretion rates over the lake are estimated as 5.5 mm yr^{-1}. Because the ice sheet approached the lake in the past at noticeably lesser velocities than it has now at Vostok, the latter accretion rates, although essentially lower than those predicted in [5, 76, 77], were sufficient to result in 215 meters of the refrozen ice. However, it should be noted that, in accordance with [85], the ice sheet thickness at Vostok may reach 3775 m and, then, the accreted ice layer is 235-m thick. This will increase the deduced ice fusion temperature by ~0.4°C and reduce the geothermal flux to $q_0 \approx 0.05$ W m^{-2}. Alternatively, a frazil formation rate of $w_f \approx 0.4$ mm yr^{-1} or a smaller non-freezing area on the island can result in the same thickness of the refrozen ice.

Another important peculiarity of the ice sheet - subglacial lake thermodynamic interaction is that the heat flux at the glacier bottom is not noticeably influenced by paleoclimatic surface temperature variations and remains practically constant with time [130]. As a consequence, the freezing rates and the accreted ice flow rate along the flow line do not vary much. Thus, the accreted ice thickness is sensitive and inversely proportional to the ice velocity which is directly related (through the total ice flow rate A) to the ice mass balance b and its paleoclimatic variations (see Eqs. (2), (3), and (9)). The present-day 215-meter thick layer of the accreted ice, being formed during ~57 kyr, mainly, under glacial conditions, has practically maximum thickness which does not exceed 220-225 m. A minimal accreted ice layer shown in Fig. 12c by the dashed curve 2 is substantially thinner after warm interglacial periods, decreasing at Vostok to 135-140 m due to much shorter time ~38 kyr of the basal ice travel across the lake.

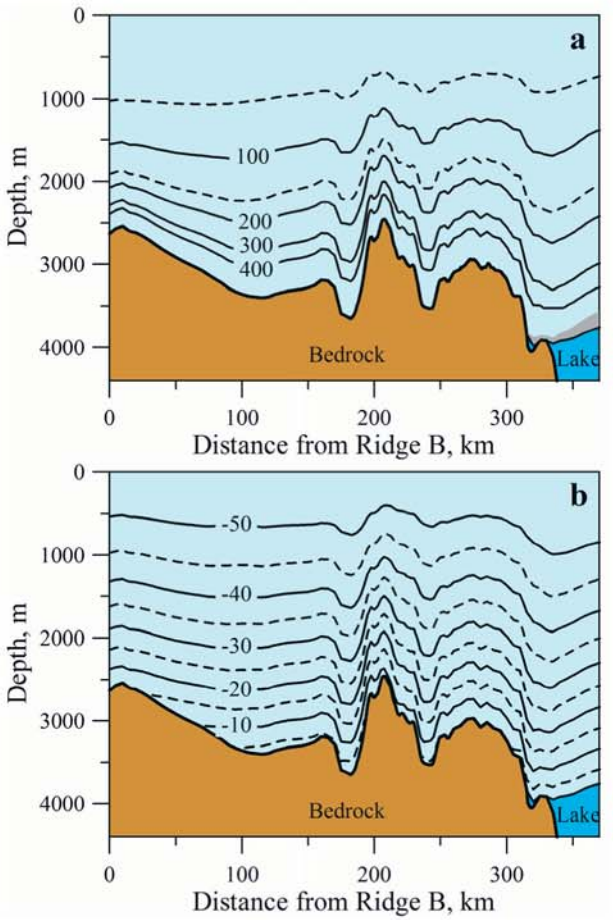

*Figure 13: Present-day ice age distribution (**a**) and temperature field (**b**) in the ice sheet along VFL. Numbers at isochrones and isotherms are ages in kyr and temperatures in °C, respectively. Accreted ice layer over the lake in (**a**) is shaded.*

The present-day ice-age distribution (isochrones) and temperature field simulated in the ice sheet body along VFL are presented in Figs. 13a and b.

6. Conclusion

This review based on the authors' publications [101, 102, 104, 112, 130, 131] demonstrates that the joint problem of ice age dating and paleoclimatic interpretation of ice core isotopic records can not be successfully solved without involving supplementary geographical, geophysical and glaciological information. A sophisticated thermo-mechanical ice flow line

model (7)-(16) and the computer system are developed and employed as a tool to infer the ice core history at Vostok through fitting the model to various data, which include the age-depth markers, borehole temperature profile, flow-line RES survey, air bubble measurements and additional available field observations. The principal issues of the paper are the constrained isotope/temperature and accumulation transfer functions (2), (3), (6) and the best-fit glaciological time scale GTS-III for the Vostok ice core (see Tables 1 and 3) simultaneously consistent with a wide spectra of all the considered experimental materials. The substantially improved modeling approaches with the more accurate and broader informational scope are believed to provide a higher reliability of the obtained results.

Acknowledgements

The authors would like to thank V.M. Kotlyakov for his encouraging and unceasing attention to our work. We thank F. Vemeux and M.J. Siegert for useful comments and also for providing the original (deuterium and deuterium excess) data from the Vostok ice core and the digitized RES record in the VFL vicinity, respectively. We are grateful to K. Cuffey, A.A. Ekaykin, F. Parrenin, J.R. Petit for numerous fruitful and stimulating discussions in the course of our research.

This work is a contribution to Project 4 of the Subprogram "Study and Research of the Antarctic", FTP "World Ocean" of the Russian Federation. It was supported from the Russian Foundation for Basic Research through the Russian-French collaboration Grant No. 05-05-66802 and the Grant No. 08-05-00464a in the Kazan State University and through the Grant No 06-05-64967a in the Arctic and Antarctic Research Institute.

References

[1] N.I. Barkov, K.V. Blinov, V.N. Petrov and A.N. Salamatin, "Chislennye experimenty po rekonstruktsii paleoklimata na osnove resul'tatov trmometrii glubokoy skvazhiny na stantsii Vostok v Antarctide. [Numerical experiments on paleoclimate reconstructions fromtemperature measurements in the deep borehole at Vostok Station in Atractica]", Mater. Glyatsiol. Issled. [Data of Glaciological Studies], **67**, 1989, pp. 116-121.

[2] N.I. Barkov and V.Ya. Lipenkov, "Nakopleniye snega v rayone stantsii Vostok, Antarktida, v 1970-1992 gg. [Snow accumulation at Vostok Station, Antarctic, 1970-1992]", Mater. Glyatsiol. Issled. [Data of Glaciological Studies], **80**, 1996, pp. 87-88.

[3] N.I. Barkov, R.N. Vostretsov, V.Ya. Lipenkov and A.N. Salamatin, "Kolebaniya temperatury voztukha I osadkov v rayone stantsii Vostok na protyazhenii chetyryeh klimaticheskih tsyklov za posledniye 420 tys. let. [Air temperature and precipitation variations in Vostok station area through four climatic cycles during recent 420 kyears]", Arktika i Antarktika [Arctic and Antarctica], 1/35, 2002, pp. 82-97.

[4] F.C. Bassinot, L.D. Labeyrie, E. Vincent, X. Quidelleur, N.J. Shackleton and Y. Lancelot, "The astronomic theory of climate and age of the Brunhes-Matuyama magnetic reversal", Earth Planet. Sci. Lett., **126**(1-3), 1994, pp. 91-108.

[5] R.E. Bell, M. Studinger, A.A. Tikku, G.K.C. Clarke, M.M. Gutner and Ch. Meertens, "Origin and fate of Lake Vostok water frozen to the base of the East Antarctic ice sheet", Nature, **416**(6878), 2002, pp. 307-310.

[6] M.L. Bender, "Orbital tuning chronology for the Vostok climate record supported by trapped gas composition", Earth Planet. Sci. Lett., **204**, 2002, pp. 275-289.

[7] M.L.Bender, G. Floch, J. Chappellaz, M. Suwa, J.-M. Barnola, T. Blunier, G. Dreyfus, J. Jouzel and F. Parrenin, "Gas age - ice age differences and the chronology of the Vostok ice core, 0 - 100 ka", J. Geophys. Res., **111**(D211115), 2006, doi: 10.1029/2005JD006488.

[8] W.F.Budd, The dynamics of ice masses, ANARE Scientific Reports. Ser A(IV) Glaciology. Antarctic Division, Dept. of Science, Publ. No.108, Melbourne, 1969.

[9] H.S. Carslaw and J.C. Jaeger, Conduction of Heat in Solids, Clarendon Press, Oxford, 1959.

[10] Ph. Ciais and J. Jouzel, "Deuterium and oxygen 18 in precipitation: isotopic model, including mixed cloud processes", J. Geophys. Res., **99**(D8), 1994, pp. 16,793-16,803.

[11] H. Craig, "Isotopic variations in meteoric waters", Science, **133**, 1961, pp. 1702-1707.

[12] H. Craig and L.I. Gordon, "Deuterium and oxygen-18 variations in the ocean and the marine atmosphere", Stable isotopes in oceanographic studies and paleotemperatures, E.Tongiorgi (Ed.), Consiglio Nazionale delle Ricerche, Laboratorio di Geologia Nucleare, Pisa, 1965, pp. 9-130.

[13] K.M. Cuffey, G.D. Clow, R.B. Alley, M. Stuiver, Ed.W. Waddington and R.W. Saltus, "Large Arctic temperature change at the Glacial-Holocene transition", Science, **270**, 1995, pp. 455-458.

[14] K.M. Cuffey and F. Vimeux, "Covariation of carbon dioxide and temperature from Vostok ice core after deuterium-excess correction", Nature, **412**(6846), 2001, pp. 523-527.

[15] Q. Dahe, J.R. Petit, J. Jouzel and M. Stievenard, "Distribution of stable isotopes in surface snow along the route of the 1990 International Trans-Antarctic Expedition", J. Glaciol., **40**(134), 1994, pp. 107-118.

[16] D. Dahl-Jensen and S.J. Johnsen, "Paleotemperatures still exist in the Greenland ice sheet", Nature, **320**(6059), 1986, pp. 250-252.

[17] D. Dahl-Jensen, K. Mosegaard, N. Grundestrup, G.D. Clow, S.J. Johnsen, A.W. Hansen and N. Balling, "Past temperatures directly from the Greenland ice sheet", Science, **282**, 1998, pp. 268-271.

[18] W. Dansgaard, "Stable isotopes in precipitation", Tellus, **16**, 1964, pp. 436-467.

[19] D.J. Drewry, Antarctic ice sheet thickness and volume. - Antarctica: Glaciological and Geophysical Folio, Scott Polar Res. Inst., Cambridge, England, U.K., 1983.

[20] D.J. Drewry and S.R. Jordan, The bedrock surface of Antarctica. - Antarctica: Glaciological and Geophysical Folio, Scott Polar Res. Inst., Cambridge, England, U.K., 1983.

[21] A.A. Ekaykin, Meteorological regime of central Antarctica and its role in the formation of isotope composition of snow thickness (Thése de Doctorat d'Etat, Université Joseph Fourier - Grenoble I), 2003.

[22] A.A. Ekaykin, V.Ya. Lipenkov, N.I. Barkov, J.R. Petit and V. Masson, "Izotopniy sostav poverhnostnogo sloya snezhnoy tolschi v rayone stanstii Vostok, Tsentral'naya Antarktida. [Isotope composition of upper part of snow layer at Vostok Station area, Central Antarctica]", Mater. Glyatsiol. Issled. [Data of Glaciological Studies], **90**, 2001, pp. 69-79.

[23] A.A. Ekaykin, V.Ya. Lipenkov, N.I. Barkov, J.R. Petit and V. Masson-Delmotte, "Spatial and temporal variability in isotope composition of recent snow in the vicinities of Vostok Station: Implications for ice-core interpretation", Ann. Glaciol., **35**, 2002, pp. 181-186.

[24] A.A. Ekaykin, V.Ya.Lipenkov, N.I. Barkov , J.R.Petit and V. Masson-Delmotte, "Pyatidesyatiletniy tsikl v izmeneniyah akkumulyatsii i izotopnogo sostava snega na stantsii Vostok. [Fifty-year cycle in variations of snow accumulation and isotope content on Vostok Station]", Mater. Glyatsiol. Issled. [Data of Glaciological Studies], **94**, 2003, pp. 163-173.

[25] E. Eriksson, "Deuterium and oxygen-18 in precipitation and other natural waters. Some theoretical considerations", Tellus, **17**, 1965, pp. 498-512.

[26] D.A. Fisher, "Remarks on the deuterium excess in precipitation in cold regions", Tellus, **43B**, 1991, pp. 401-407.

[27] J.R.Gat and R. Gonfiantini (Eds). Stable Isotope Hydrology. Deuterium and oxygen-18 in the water cycle, Technical Reports Series No.210, International Atomic Energy Agency, Vienna, 1981.

[28] V.N. Golubev, V.N. Konischev, S.A. Sokratov and P.B.Grebennikov, "Izmeneniya izotopnogo sostava sezonnogo snezhnogo pokrova v protsesse sublimatsii. [Isotopic content changes in seasonal snow cover due to sublimation]", Materials of the 2-d conference of geocryologists of Russia, v.2: Dynamic Geocryology, Publishing House of the Moscow State University, Moscow, 2001, pp.106-115.

[29] C. Goujon, J.-M. Barnola and C. Ritz, "Modeling the densification of polar firn including heat diffusion: Application to close-off characteristics and gas isotopic fractionation for Antarctica and Greenland sites", J. Geophys. Res., **108**(D24), 2003, pp. 4792-4809.

[30] A.J. Gow, "Bubbles and bubble pressures in Antarctic glacier ice", J. Glaciol., **7**(50), 1968, pp.167-182.

[31] S.S. Grigoryan, M.S. Krass and P.A. Shumskiy, "Mathematical model of a three dimensional non-isothermal glacier", J. Glaciol., **7**(77), 1976, pp.401-417.

[32] M.B. Hendricks, D.J.D. Paolo and R.C. Cohen, "Space and time variations of $\delta^{18}O$ and δD in precipitation: can paleotemperature be estimated from ice cores?", Global Biogeochemical Cycles, **14**(3), 2000, pp. 851-861.

[33] P.V. Hobbs, Ice Physics, Clarendon Press, Oxford, 1974.

[34] T. Hondoh, H. Shoji, O. Watanabe, A.N. Salamatin and V.Ya. Lipenkov, "Depth-age and temperature prediction at Dome Fuji station, East Antarctica", Ann. Glaciol, **35**, 2002, pp. 384-390.

[35] T.Hondoh, H.Shoji, O.Watanabe, E.A. Tsyganova, A.N. Salamatin and V.Ya. Lipenkov, "Average time scale for Dome Fuji ice core, East Antarctica", Polar Meteorol. Glaciol., **18**, 2004, pp. 1-18.

[36] J. Imbrie, J.D. Hays , D.G. Martinson, A. McIntyre, A.C. Mix, J.J. Morley, N.G. Pisias, W.L. Prell and N.J. Shackleton, "The orbital theory of Pleistocene climate: support from a revised chronology of the marine $\delta^{18}O$ record", Milankovich and Climate. Part 1, A.L. Berger et al. (Eds.), D. Reidel Publishing Company, 1984, pp. 269-305.

[37] S.J. Johnsen, D. Dahl-Jensen, W. Dansgaard, N. Grundestrup, "Greenland paleotemperatures derived from GRIP borehole temperature and ice-core isotope profiles", Tellus, **47B**(5), 1995, pp. 624-629.

[38] S.J. Johnsen, W. Dansgaard and J.W.C. White, "The origin of Arctic precipitation under present and glacial conditions", Tellus, **41B**, 1989, pp. 452-468.

[39] J. Jouzel, R.B. Alley, K.M. Cuffey and 10 others, "Validity of temperature reconstruction from water

isotopes in ice cores", J. Geophys. Res., **102**(C12), 1997, pp.26,471-26,487.

[40] J. Jouzel, N.I. Barkov, J.M. Barnola and 14 others, "Extending the Vostok ice-core record of paleoclimate to the penultimate glacial period", Nature, **364**(6436), 1993, pp. 407-412.

[41] J. Jouzel, C. Lorius, J.R. Petit, C. Genton, N.I. Barkov, V.M. Kotlyakov and V.N. Petrov, "Vostok ice core: A continuous isotope temperature record over the last climatic cycle (160,000 years)", Nature, **329**(6138), 1987, pp. 403-408.

[42] J. Jouzel and L. Merlivat, "Deuterium and oxygen 18 in precipitation: modeling of the isotopic effects during snow formation", J. Geophys. Res., **89**(D7), 1984, pp.11,749-11,757.

[43] J. Jouzel, L. Merlivat and C. Lorius, "Deuterium excess in an East Antarctic ice core suggests higher humidity at the ocean surface during the last glacial maximum", Nature, **299**(5885), 1982, pp. 688-691.

[44] J. Jouzel, J.R.Petit, R. Souchez, N.I. Barkov, V.Ya. Lipenkov, D. Raynaud, M. Stievenard, N.I. Vassiliev, V. Verbeke and V. Vimeux, "More than 200 meters of lake ice above subglacial Lake Vostok, Antarctica", Science, **286**, 1999, pp.2138-2141.

[45] J. Jouzel, F. Vimeux, N. Caillon, G. Delaygue, G. Hoffmann, V. Masson-Delmotte and F. Parrenin, "Magnitude of isotope/temperature scaling for interpretation of central Antarctic ice cores", J. Geophys. Res., 2003, **108**(D12), pp. 4361-4370, doi: 10.1029/2002JD002677.

[46] A.P. Kapitsa, J.R. Ridley, G. de Q. Robin, M.J. Siegert and I.A. Zotikov, "A large deep freshwater lake beneath the ice of central East Antarctica", Nature, **381**, 1996, pp. 684-686.

[47] J.L. Kavanaugh and K.M. Cuffey, "Generalized view of source-region effects on δD and deuterium excess of ice-sheet precipitation", Ann. Glaciol., **35**, 2002, pp. 111-117.

[48] J.L. Kavanaugh and K.M. Cuffey, "Space and time variation of $\delta^{18}O$ and δD in Antarctic precipitation revisited", Global Biogeochemical Cycles, **17**(1), 2003, pp. 1017-1030.

[49] V.N. Konishchev, V.N. Golubev and S.A. Sokratov, "Sublimation from a seasonal snow cover and an isotopic content of ice wedges in the light of a palaeoclimate reconstruction", Permafrost (ICOP 2003: Proc. 8th Int. Conf. Permafrost, 21-25 July 2003, Zu"rich, Switzerland), Vol. 1, M. Phillips, S.M. Springman and L.U. Arenson (Eds.), A.A. Balkema Publishers, Lisse, etc., 2003, pp. 585-590.

[50] V.M. Kotlyakov and F.G. Gordienko, Izotopnaya i geohimicheskaya glyatsiologiya [Isotopic and geochemical glaciology], Gidrometeoizdat, Leningrad, 1982.

[51] J.M. Landwehr and I.J. Winograd, "Dating the Vostok ice core record by importing the Devils Hole chronology", J. Geophys. Res., **106**(D23), 2001, pp. 31,837-31,851.

[52] G.J.-M.C. Leysinger Vieli, M.J. Siegert and A.J. Payne, "Reconstructing ice sheet accumulation rates at Ridge B, East Antarctica", Ann. Glaciol., **39**, 2004, pp. 326-330.

[53] V.Ya. Lipenkov, A.A. Ekaykin, N.I. Barkov and M. Pourshet, "O svyazi plotnosti poverhnostnogo sloya snega v Antarktide so skorostyu vetra. [On connection of density of surface ice layer in Antarctica with wind velocity]", Mater. Glyatsiol. Issled. [Data of Glaciological Studies], **85**, 1998, pp. 148-158.

[54] V.Ya. Lipenkov and V.A. Istomin, "On stability of air clathrate-hydrate crystals in subglacial lake Vostok, Antarctica", Mater. Glyatsiol. Issled. [Data of Glaciological Studies], **91**, 2001, pp. 138-149.

[55] V.Ya. Lipenkov, O.A. Ryskin and N.I. Barkov, "O svyazi mezhdu kolichestvom vozdushnyh vklyucheniy vo l'du i usloviyami l'doobrazovaniya. [Relationship of number of air inclusions in ice with ice formation conditions]", Mater. Glyatsiol. Issled. [Data of Glaciological Studies], **86**, 1999, pp. 75-91.

[56] V.Ya. Lipenkov and A.N. Salamatin, "Past accumulation rates from air bubble number count in the Vostok and EPICA DC ice cores", J. Glaciol., 2008 (submitted).

[57] V.Ya. Lipenkov, A.N. Salamatin and P. Duval, "Bubbly ice densification in ice sheets: II Applications", J. Glaciol., **43**(145), 1997, pp. 397-407.

[58] V.Ya.Lipenkov, A.N. Salamatin, P.Duval, H. Ohno and T. Hondoh, "LGM accumulation - temperature relationship from air bubble studies in EPICA DC, Vsotok, and Dome Fuji ice cores", Geophys. Res. Abstracts, Vol. 7, Abstract No. 11040, European Geosciences Union, 2005.

[59] V.Ya. Lipenkov, Yu.A. Shibaev, A.N. Salamatin, A.A. Ekaykin, R.N. Vostretsov and A.V. Preobrazhenskaya, "Sovremennye klimaticheskie izmeneniya, zaregistrirovannye v variatsiyah temperatury verhnego 100-metrovogo sloya lednikovoy tolschi na stantsii Vostok. [Current climate changes recorded in ice temperature variations in upper 100-m layer, Vostok Station area]", Mater. Glyatsiol. Issled. [Data of Glaciological Studies], **97**, 2004, pp. 44-56.

[60] H. Liu, K. Jezek, B. Li and Z. Zhao, "Radarsat Antarctic Mapping Project digital elevation model version 2", CO: National Snow and Ice Data Center. Digital media, Boulder, 2001.

[61] L. Lliboutry, "A critical review of analytical approximate solutions for steady state velocities and temperatures in cold ice sheets", Z. Gletscherkd. Glazealgeol., **15**(2), 1979, pp. 135-148.

[62] C. Lorius and L. Merlivat, "Distribution of mean surface stable isotope values in East Antarctica: observed changes with depth in the coastal area", Isotopes and Impurities in Snow and Ice, IAHS Publ. 118, 1977, pp. 127-137.

[63] K.R. Ludwig, K.R. Simmons, B.J. Szabo, I.J. Winograd, J.M. Landwehr, A.C. Riggs and R.J. Hoffman, "Mass-spectrometric ^{230}Th-^{234}U-^{238}U dating of the Devils Hole calcite vein", Science, **258**(5080), 1992, pp. 284-287.

[64] V.V. Lukin, V.N. Masolov, A.V. Mironov, A.M. Popkov, S.V. Popov, A.N. Sheremetyev, S.R. Verkulich and I.N. Kuzmina, "Rezul'taty geofizicheskih issledovaniy podlednikovogo ozera Vostok (Antarktida) v 1995-1999 gg. [The results of geophysical research of the subglacial Vostok lake (Antarctica) for the period 1995-1999]", Problemy Arktiki i Antarktiki [Problems of Arctic and Antarctic], **72**, 2000, pp. 237-248.

[65] M.B. Lythe, D.G. Vaughan and BEDMAP Consortium, "BEDMAP: A new ice thickness and subglacial topographic model of Antarctica", J. Geophys. Res., **106**(B6), 2001, pp. 11,335-11,351.

[66] V.N. Masolov, V.V. Lukin, A.N. Sheremetyev and S.V. Popov, "Geofizicheskie issledovaniya podlednikovogo ozera Vostok v Vostochnoy Antarktide. [Geophysical investigations of the subglacial lake Vostok in Eastern Antarctica]", Doklady Akademii Nauk, **379**(5), 2001, pp. 680-685. [Transl.: Doklady Earth Sciences, **379A**(6), 2001, pp. 734-738].

[67] V.N. Masolov, S.V. Popov, V.V. Lukin, A.N. Sheremetyev and A.M. Popkov, "Russian geophysical studies of Lake Vostok, Central East Antarctica", Antarctica - Contributions to Global Earth Sciences, D.K. Fütterer, D. Damaske, G. Kleinschmidt, H. Miller and F. Tessensohn (Eds.), Springer, Berlin, Heidelberg, New York, 2006, pp. 135-140.

[68] C.P. McKay, K.P. Hand, P.T. Doran, D.T. Anderson and J.C. Priscu, "Clathrate formation and the fate of noble and biologically useful gases in Lake Vostok, Antarctica", Geophys. Res. Lett., **30**(13), 2003, pp. 1702-1705.

[69] L. Merlivat and J. Jouzel, "Global climatic interpretation of the deuterium-oxygen 18 relationship for precipitation", J. Geophys. Res., **84**(C8), 1979, pp. 5029-5033.

[70] K. Mosegaard, "Resolution analysis of general inverse problems through inverse Monte Carlo sampling", Inverse Problems, **14**(1), 1998, pp. 405-426.

[71] K. Mosegaard and A. Tarantola, "Monte Carlo sampling of solutions to inverse problems", J. Geophys. Res., **100**(B7), 1995, pp. 12,431-12,447.

[72] O.V. Nagornov and Yu.V. Konovalov, "Chuvstvitel'nost' metodov rekonstruktsii temperatury poverhnosti lednikov k pogreshnostyam izmereniy i stepeni neopredelennosti vhodnyh parametrov v modeli. [Sensitivity of methods of glacier surface temperature reconstruction to errors of measurements and degree of uncertainty of model data input]", Mater. Glyatsiol. Issled. [Data of Glaciological Studies], **92**, 2002, pp. 201-215.

[73] S.A. Nickolayev, N.G. Nickolayeva and A.N.Salamatin, Teplofizika gornyh porod. [Thermophysics of rocks], Publishing House of Kazan Univ., Kazan, 1987.

[74] F. Parrenin, J. Jouzel, C. Waelbroeck, C. Ritz and J.M. Barnola, "Dating the Vostok ice core by inverse method", J. Geophys. Res., **106**(D23), 2001, pp. 31,837-31,851.

[75] F. Parrenin, F. Remy, C. Ritz, M. Siegert and J. Jouzel, "New modeling of the Vostok ice flow line and implications for the glaciological chronology of the Vostok ice core", J. Geophys. Res., **109**(D20102), 2004, doi:10.1029/2004JD004561.

[76] J.R. Petit, "Ice water exchanges in Lake Vostok constrained by an energy balance model", Geophys. Res. Abstracts (EGS - AGU - EUG Joint Assembly, Nice, France, April, 2003), Vol. 5, Abstract No. 03628, European Geophysical Society, 2003.

[77] J.R. Petit, I. Alekhina and S.A. Bulat, "Lake Vostok, Antarctica: Exploring a Subglacial Lake and Searching for Life in an Extreme Environment", Lectures in Astrobiology, Vol. 1, Series: Advances in Astrobiology and Biogeophysics, M. Gargaud, B. Barbier, H. Martin, J. Reisse (Eds.), Springer, 2005, pp.227-288.

[78] J.R. Petit, J. Jouzel, D. Raynaud and 16 others, "Climate and atmospheric history of the past 420,000 years from the Vostok ice core, Antarctica", Nature, **399**(6735), 1999, pp. 429-436.

[79] J.R. Petit, J.W.C. White, N.W. Young, J. Jouzel and Y.S. Korotkevich, "Deuterium excess in recent Antarctic snow", J. Geophys. Res., **96**(D3), 1991, pp. 5113-5122.

[80] H.R. Phillpot and J.W. Zillman, "The surface temperature inversion over the Antarctic Continent", J. Geophys. Res., **75**(21), 1970, pp. 4161-4169.

[81] S.V. Popov, V.V. Kharitonov and Yu.B. Chernoglazov, "Plotnost' I udel'naya akkumulyatsiya snezhnogo pokrova v yuzhnoy chasti podlednikovogo ozera Vostok (Vostochnaya Antarktida). [Density and specific snow accumulation in southern part of Vostok subglacial lake area (Eastern Antarctica)]", Mater. Glyatsiol.

Issled. [Data of Glaciological Studies], **96**, 2004, pp. 201-206.

[82] S.V.Popov, G.L.Leitchenkov, M.Yu. Moskalevsky, V.V. Kharitonov, V.N. Masolov and BEDMAP Consortium, "ABRIS Project: new bedrock topography map for central Antarctica", Proc. 10th ISAES, A.K. Cooper, C.R. Raymond et al. (Eds.), USGS Open-File Report 2007-1047, Extended Abstract No.026, 2007.

[83] S.V. Popov and V.N. Masolov, "Forty-seven new subglacial lakes in the 0°-110° sector of East Antarctica", J. Glaciol., **53**(181), 2007, pp. 289-297.

[84] S.V. Popov, A.N. Sheremetyev, V.N. Masolov and V.V. Lukin, "Osnovnye rezul'taty nazemnogo radiolokatsionnogo profilirovaniya v rayone podlednikovogo ozera Vostok v 1998-2002 gg. [Main results of ground radio-echo sounding in the area of subglacial Vostok Lake, 1998-2002]", Mater. Glyatsiol. Issled. [Data of Glaciological Studies], **94**, 2003, pp. 187-193.

[85] S.V. Popov, A.N. Sheremetyev, V.N. Masolov, V.V. Lukin, A.V. Mironov and V.S. Luchininov, "Velocity of radio-wave propagation in ice at Vostok station, Antarctica", J. Glaciol., **49**(165), 2003, pp. 179-183.

[86] V.Yu. Potapenko and A.N. Salamatin, "Obschaya matematicheskaya model' kvazistatsionarnogo lednikovogo pokrova. [A general mathematical model of a quasi-stationary ice sheet]", Problemy Arktiki i Antarktiki [Problems of Arctic and Antarctic], **59**, 1985, pp. 21-26.

[87] V.Yu. Potapenko and A.N. Salamatin, "Kriterial'niy analiz uravneniy, opisyvayuschih termodynamicheskie protsessy v lednikovyh pokrovah. [Scale analysis of equations governing thermodynamic processes in ice sheets]", Problemy Arktiki i Antarktiki [Problems of Arctic and Antarctic], **59**, 1985, pp. 74-77.

[88] G.M. Raisbeck, F. Yiou, D. Bourles, C. Lorius, J. Jouzel and N.I. Barkov, "Evidence for two intervals of enhanced ^{10}Be deposition in Antarctic ice during the last glacial period", Nature, **326**, 1987, pp. 273-277.

[89] D. Raynaud, J.-M.Barnola, R. Souchez, R. Lorrian, J.R. Petit, P. Duval and V.Ya. Lipenkov, "The record for marine isotopic stage 11", Nature, **436**, 2005, pp. 39-40.

[90] D. Raynaud, V.Ya Lipenkov, B. Lemieux-Dudon, P. Duval, M.-F. Loutre and N. Lhomme, "The local insolation signature of air content in Antarctic ice. A new step toward an absolute dating of ice records", Earth Planet. Sci. Lett., **261**, 2007, pp. 337-349.

[91] N. Reeh, "A flow-line model for calculating the surface profile and the velocity, strain rate, and stress fields in an ice sheet", J. Glaciol., **34**(116), 1988, pp. 46-54.

[92] F. Rémy, P. Shaeffer, B. Legrésy, "Ice flow physical processes derived from the ERS-1 high-resolution map of the Antarctica and Greenland ice sheets", Geophys. J. Int., **139**, 1999, pp.645-656.

[93] C. Ritz, "Time dependent boundary conditions for calculations of temperature fields in ice sheets", The Physical Basis of Ice Sheet Modeling, IAHS Publ. No.170, 1987, pp. 208-216.

[94] C. Ritz, "Interpretation of the temperature profile measured at Vostok. East Antarctica", Ann. Glaciol., **12**, 1989, pp.138-144.

[95] C. Ritz, Un modèle thermo-mecanique d'évolution pour le bassin glaciaire Antarcique Vostok – glacier Byrd: sensibilité aux valeurs des paramèters mal connus (Thése de Doctorat d'Etat. Université Joseph Fourier – Grenoble I), 1992.

[96] C. Ritz, V. Rommelaere and C. Dumas, "Modeling the evolution of Antarctic ice sheet over the last 420,000 years: Implications for altitude changes in the Vostok region", J. Geophys. Res., **106**(D23), 2001, pp.31,943-31,964.

[97] G. de Q. Robin, "Ice cores and climatic changes", Phill. Trans. R. Soc. London, **280**(**B**), 1977, pp. 143-168.

[98] G. de Q. Robin, D.J. Drewry and D. T. Meldrum, "International studies of ice sheet and bedrock", Phill. Trans. R. Soc. London, **279(B)**, 1977, pp. 185-196.

[99] A.N. Salamatin, "Analiz prosteyshih matematicheskih modeley kupolovidnyh lednikov. [Analysis of the simplest mathematical models of copular glaciers]", Issled. Priklad. Matem. [Studies in Applied Mathematics], **7**, Publish. House of Kazan Univ., Kazan, 1979, pp. 131-139. [Transl.: J. Sov. Math., **43**(3), 1988, pp. 2506-2512].

[100] A.N. Salamatin, "Ice sheet modelling taking account of glacier ice compressibility", Glaciers-Ocean-Atmosphere Interactions, IAHS Publ. No. 208, 1991, pp. 183-192.

[101] A.N. Salamatin, "Paleoclimatic reconstructions based on borehole temperature measurements in ice sheets. Possibilities and limitations", Physics of Ice Core Records, T. Hondoh (Ed.), Hokkaido University Press, Sapporo, 2000, pp. 243-282.

[102] A.N. Salamatin, A.A.Ekaykin and V.A. Lipenkov, "Modelling isotopic composition in precipitation in Centeral Antarctica", Mater. Glyatsiol. Issled. [Data of Glaciological Studies], **97**, 2004, pp. 24-34.

[103] A.N. Salamatin and V.Ya. Lipenkov, "Simple relations for the close-off depth and age in dry snow densification", Ann. Glaciol, **49**, 2008, in press.

[104] A.N. Salamatin, V.Ya. Lipenkov, N.I. Barkov, J. Jouzel, J.R. Petit and D. Raynaud, "Ice core age dating and paleothermometer calibration based on isotope and temperature profiles from deep boreholes at Vostok Station (East Antarctica)", J. Geophys. Res., **103**(D8), 1998, pp. 8963-8977.

[105] A.N. Salamatin, V.Ya. Lipenkov, J.-M. Barnola, A. Hori, P. Duval and T. Hondoh, "Snow-firn densification in polar ice sheets", Physics of Ice Core Records, Vol. 2, T. Hondoh (Ed.), Hokkaido University Press, Sapporo, 2008 (this issue).

[106] A.N. Salamatin, V.Ya.Lipenkov and K.V. Blinov, "Vostok (Antarctica) climate record time-scale deduced from the analysis of a borehole-temperature profile", Ann. Glaciol., **20**, 1994, pp. 207-214.

[107] A.N. Salamatin, V.Ya.Lipenkov and K.V. Blinov, "Vosstanovlenie klimaticheskih izmeneniy temperatury na poverhnosti antarkticheskogo lednikovogo pokrova v proshlom po rezul'tatam temperaturnyh izmereniy v glubokih skvazhinah na stantsii Vostok. [Reconstruction of temperature climatic variations on the Antarctic ice sheet in the past from temperature measurements in deep boreholes at Vostok Station]", Mater. Glyatsiol. Issled. [Data of Glaciological Studies], **79**, 1995, pp. 59-64 [Transl.: Mater. Glyatsiol. Issled., **81** (IAHS Symp. at Tashkent 1993 - Seasonal and Long-Term Fluctuations of Nival and Glacial Processes in Mountains at Different Scales of Analysis), 1997, pp. 141-146].

[108] A.N. Salamatin, V.Ya. Lipenkov and T. Hondoh, "Air-hydrate crystal growth in polar ice", J. Crystal Growth, 257, 2003, pp. 412-426.

[109] A.N. Salamatin, J.R. Petit and V.Ya. Lipenkov, "An estimate of LV isolation time from a sensitivity experiment for the melting area", Geophys. Res. Abstracts (EGS - AGU - EUG Joint Assembly, Nice, France, April, 2003), Vol. 5, Abstract No.08277, European Geophysical Society, 2003.

[110] A.N. Salamatin and C. Ritz, "A simplified multi-scale model for predicting climatic variations of the ice sheet surface elevation in the Central Antarctica", Ann. Glaciol., **23**, 1996, pp. 28-35.

[111] A.N. Salamatin, T. Shiraiwa, Ya.D. Muravyev and M.F. Ziganshin, "Heat transfer in the seasonal active layer of Gorshkov ice cap on the summit of Ushkovsky volcano, Kamchatka Peninsula", Bulletin of Glaciological Research (Japanese Society of Snow and Ice), 19, 2002, pp. 47-52.

[112] A.N.Salamatin, E.A. Tsyganova, V.Ya. Lipenkov and J.R. Petit, "Vostok (Antarctica) ice-core time scale from datings of different origins", Ann. Glaciol., **39**, 2004, pp. 283-292.

[113] A.N. Salamatin, R.N. Vostretsov, J.R. Petit, V.Ya. Lipenkov and N.I. Barkov, "Geophysical and paleoclimatic implications of the stacked temperature profile from the deep borehole at Vostok Station (Antarctica)", Mater. Glyatsiol. Issled. [Data of Glaciological Studies], **85**, 1998, pp. 233-240.

[114] K. Satow, O. Watanabe, H. Shoji and H. Motoyama, "The relationship among accumulation rate, stable isotope ratio and surface temperature on the East Dronning Maud Land, Antarctica", Polar Meteorol. Glaciol., **13**, 1999, pp. 43-52.

[115] M. Schneebeli and S.A. Sokratov, "Tomography of temperature gradient metamorphism of snow and associarted changes in heat conductivity", Hydrological Processes, **18**, 2004, pp. 3655-3665.

[116] M.J. Siegert and J.A. Dowdeswell, "Spatial variations in heat at the base of the Antarctic ice sheet from analysis of the thermal regime above subglacial lakes", J. Glaciol., **42**(142), 1996, pp. 501-509.

[117] M.J. Siegert, J.C. Ellis-Evans, M. Tranter, Ch. Mayer, J.R. Petit, A. Salamatin and J.C. Priscu, "Physical, chemical and biological processes in Lake Vostok and other Antarctic subglacial lakes", Nature, **414**(6864), 2001, pp. 603-609.

[118] M.J. Siegert and R. Kwok, "Ice-sheet radar layering and the development of preferred crystal orientation fabrics between Lake Vostok and Ridge B, central East Antarctica", Earth Planet. Sci. Lett., **179**(2), 2000, pp. 227-235.

[119] M.J. Siegert and J.K. Ridley, "An analysis of the ice-sheet surface and subsurface topography above the Vostok Station subglacial lake, central East Antarctica", J. Geophys. Res., **103**(B5), 1998, pp.10,195-10,207.

[120] J.C. Simões, J.R. Petit, R. Souchez, V.Ya. Lipenkov, M. de Angelis, L. Liu, J. Jouzel and P. Duval, "Evidence of glacial flour in the deepest 89 m of the Vostok glacier ice core", Ann. Glaciol., **35**, 2002, pp. 340-346.

[121] G.A. Slack, "Thermal conductivity of ice", Physical Review B, **22**(6), 1980, pp. 3065-3071.

[122] R. Souchez, J.R. Petit, J. Jouzel, M. de Angelis and J.-L. Tison, "Reassessing Lake Vostok's behaviour from existing and new ice core data", Earth Planet. Sci. Lett., **217**, 2003, pp. 163-170.

[123] T. Sowers, M. Bender, L. Laberyrie, D. Martinson, J. Jouzel, D. Raynaud, J.J. Pichon and Y.S. Korotkevich, "A 135,000-year Vostok-SPECMAP common temporal framework", Paleoceanography, **8**(6), 1993, pp. 737-766.

[124] M.K. Spencer, R.B. Alley and J.J. Fitzpatrick, "Developing a bubble number-density paleoclimate indicator for glacier ice", J. Glaciol., **52**(178), 2006, pp.358-364.

[125] M. Studinger, R.I. Bell, G.D. Karner and 9 others, "Ice cover, landscape setting, and geological framework of Lake Vostok, East Antarctica", Earth Planet. Sci. Lett., **205**, 2003, pp. 195-210.

[126] M. Sturm, J. Holmgren, M. König and K. Morris, "The thermal conductivity of seasonal snow", J. Glaciol., **43**(143), 1997, pp. 26-41.

[127] I.E. Tabacco, C. Bianchi, A. Zirizzotti, E. Zuccheretti, A. Forieri and A. Della Vedova, "Airborne radar survey above Vostok region, east-central Antarctica: ice thickness and Lake Vostok geometry", J. Glaciol., **48**(160), 2002, pp. 62-69.

[128] A. Tarantola, Inverse Problem Theory: Methods for Data Fitting and Model Parameter Estimation, Elsevier Science, New York, 1987.

[129] A.A. Tikku, R.E. Bell, M. Studinger and G.K.C. Clarke, "Ice flow field over Lake Vostok, East Antarctica inferred by structure tracking", Earth Planet. Sci. Lett., **207**, 2004, pp. 249-261.

[130] E.A. Tsyganova and A.N. Salamatin, "Non-stationary temperature field simulations along the ice flow line "Ridge B - Vostok Station", East Antarctica", Mater. Glyatsiol. Issled. [Data of Glaciological Studies], **97**, 2004, pp. 57-70.

[131] E.A. Tsyganova and A.N. Salamatin, "Paleoklimaticheskaya interpretatsiya izotopnogo sostava i vozrast ledyanogo kerna so stantsii Vostok, Tsentral'naya Antarktida. [Pelaoclimatic interpretation of isotopic content and age dating of the ice core from Vostok Station, Central Antarctica]", Mater. Glyatsiol. Issled. [Data of Glaciological Studies], **100**, 2006, pp. 5-23.

[132] E.A. Tsyganova, A.N. Salamatin and V.Ya. Lipenkov, "Modelirovanie protsessa rosta vozdushnyh gidratov v lednikovom pokrove Antarktidy. [Modelling air-hydrate growth process in Antarctic ice sheet]", Materials of the 3-d conference of geocryologists of Russia (MSU, June 1-3, 2005), Vol.1, Publishing House of the Moscow State University, Moscow, 2005, pp.286-292.

[133] Yu.K. Vasilchuk and V.M. Kotlyakov, Osnovy izotopnoy geokriologii i glyatsiologii [The principles of isotopic geocryology and glaciology], Publishing House of the Moscow State University, Moscow, 2000.

[134] F. Vimeux, K.M. Cuffey and J. Jouzel, "New insights into Southern Hemisphere temperature changes from Vostok ice cores using deuterium excess correction", Earth Planet. Sci. Lett., **203**, 2002, pp. 830-843.

[135] F. Vimeux, V. Masson, G. Delaygue, J. Jouzel, J.R. Petit and M. Stievenard, "A 420,000 year deuterium excess record from East Antarctica: Information on past changes in the origin of precipitation at Vostok", J. Geophys. Res., **106**(D23), 2001, pp.31,863-31,873.

[136] R.N. Vostretsov, D.N. Dmitriev, O.F. Putikov, K.V. Blinov and S.V. Mitin, "Osnovnye resul'taty geofizicheskih issledovaniy glubokih skvazhin i ledyanogo kerna v Vostochnoy Antarktide. [Main results of geophysical studies of deep boreholes and ice core in East Antarctica]", Mater. Glyatsiol. Issled. [Data of Glaciological Studies], **51**, 1984, pp. 172-178.

[137] O. Watanabe, J. Jouzel, S. Johnsen, F. Parrenin, H. Shoji and N. Yoshida, "Homogeneous climate variability across East Antarctica over the past three glacial cycles", Nature, **422**(6931), 2003, pp. 509-512.

[138] J. Wendt, R. Dietrich, M. Fritsche, A. Wendt, A. Yuskevich, A. Kokhanov, A. Senatorov, V. Lukin, K. Shibuya and K. Doi, "Geodetic observations of ice flow velocities over the southern part of subglacial Lake Vostok, Antarctica, and their glaciological implications", Geophys. J. Int., **166**, 2006, pp. 991-998.

[139] I.J. Winograd, T.B.Coplen, J.M. Landvehr, A.C. Riggs, K.R. Ludwig, B.J. Szabo, P.T. Kolesar and K.M. Revesz, "Continuous 500,000-year climate record from vein calcite in Devils Hole, Nevada", Science, **258**(5080), 1992, pp.255-260.

[140] I.J. Winograd, J.M. Landvehr, K.R. Ludwig, T.B.Coplen and A.C. Riggs, "Duration and structure of the past four interglaciations", Quat. Res., **48**(2), 1997, pp.141-154.

[141] P. Yiou, K. Fuhrer, L.D. Meeker, J. Jouzel, S. Johnsen and P.A. Mayewski, "Paleoclimatic variability inferred from the spectral analysis of Greenland and Antarctic ice-core data", J. Geophys. Res., **102**(C12), 1997, pp. 26,441-26,454.

[142] F. Yiou, G.M. Raisbeck, S. Baumgartner and 9 others,"Beryllium 10 in the Greenland Ice Core Project ice core at Summit, Greenland", J. Geophys. Res., **102**(C12), 1997, pp. 26,783-26,794.